

1 **A Central Asia Hydrologic Monitoring Dataset for Food and**
2 **Water Security Applications in Afghanistan**

3 Amy L. McNally^{1,2,3}, Jossy Jacob^{1,4}, Kristi Arsenault^{1,2}, Kimberly Slinski^{1,5}, Daniel P. Sarmiento^{1,2},
4 Andrew Hoell⁶, Shahriar Pervez⁷, James Rowland⁸, Mike Budde⁸, Sujay Kumar¹, Christa Peters-
5 Lidard¹, James P. Verdin³

6

7 1 NASA Goddard Space Flight Center, Greenbelt, MD, 20771, United States

8 2 Science Applications International Corporation Inc., Reston, VA, 20190, United States

9 3 U.S. Agency for International Development, Washington, DC, 20523, United States

10 4 Science Systems and Applications Inc., Lanham, MD, 20706, United States

11 5 University of Maryland Earth Systems Science Interdisciplinary Center, College Park, MD,
12 20740, United States

13 6 National Oceanic and Atmospheric Administration, Physical Science Laboratory, Boulder, CO,
14 80305, United States

15 7 Arctic Slope Regional Corporation Federal Data Solutions, Contractor to U.S. Geological Survey,
16 Earth Resources Observation and Science (EROS) Center, Sioux Falls, SD, 57198, United States

17 8 U.S. Geological Survey, EROS Center, Sioux Falls, South Dakota, 57198, United States

18

19 *Correspondence to:* Amy L. McNally (amy.l.mcnally@nasa.gov)

20 **Abstract**

21
22 From the Hindu Kush Mountains to the Registan desert, Afghanistan is a diverse landscape where
23 droughts, floods, conflict, and economic market accessibility pose challenges for agricultural
24 livelihoods and food security. The ability to remotely monitor environmental conditions is critical to
25 support decision making for humanitarian assistance. The Famine Early Warning Systems Network
26 (FEWS NET) Land Data Assimilation System (FLDAS) global and Central Asia data streams
27 provide information on hydrologic states for routine integrated food security analysis. While
28 developed for a specific project, these data are publicly available and useful for other applications
29 that require hydrologic estimates of the water and energy balance. These two data streams are
30 unique because of their suitability for routine monitoring, as well as a historical record for
31 computing relative indicators of water availability. The global stream is available at ~1 month
32 latency, monthly average outputs on a 10-km grid from 1982-present. The second data stream,
33 Central Asia (30-100 °E, 21-56 °N), at ~1 day latency, provides daily average outputs on a 1-km
34 grid from 2000-present. This paper describes the configuration of the two FLDAS data streams,
35 background on the software modeling framework, selected meteorological inputs and parameters,
36 and results from previous evaluation studies. We also provide additional analysis of precipitation
37 and snow cover over Afghanistan. We conclude with an example of how these data are used in
38 integrated food security analysis. For use in new and innovative studies that will improve
39 understanding of this region, these data are hosted by U.S. Geological Survey data portals and the
40 National Aeronautics and Space Administration (NASA). The Central Asia data described in this
41 manuscript can be accessed via the NASA repository at 10.5067/VQ4CD3Y9YC0R, the global data
42 described in this manuscript can be accessed via the NASA repository at 10.5067/5NHC22T9375G.

43 **1 Introduction**

44 From the Hindu Kush Mountains to the Registan desert, Afghanistan is a diverse landscape where
45 droughts, floods, conflict, and economic market accessibility pose challenges for agricultural
46 livelihoods and food security. The ability to remotely monitor environmental conditions is critical to
47 support decision making for economic development, humanitarian assistance, water resource
48 management, agriculture and more. Environmental datasets can be combined with socio-economic
49 variables and transformed into customized products to support decision making. This is the
50 definition of a ‘climate service’ (Hewitt et al., 2012).

51
52 Hydrologic and land surface datasets are particularly relevant for agriculture and water resources
53 decision making. When these datasets are credible, updated routinely, and made publicly available,
54 the influences of climate variability and climate change can be incorporated into specialized
55 analyses by intermediary users¹. One example of an intermediary user central to this data descriptor
56 is the food security analysts of the Famine Early Warning Systems Network (FEWS NET). FEWS

¹ The WMO defines intermediate (intermediary) users as those who transform climate information into a climate service

57 NET analysts combine environmental information, largely from remote sensing and earth system
58 models, with information on nutrition, livelihoods, markets, and trade to provide decision support to
59 the U.S. Agency for International Development (USAID) Bureau of Humanitarian Assistance.
60 Additional examples and discussion of the production of climate service inputs can be found in the
61 literature (e.g., Vincent et al., 2018; McNally et al., 2019).

62
63 While these data are tailored to specific needs, they are also applicable to other climate services and
64 research e.g., desert locusts movement forecasting (Tabar et al., 2021). To that end, this paper
65 describes the FEWS NET Land Data Assimilation System (FLDAS) global and Central Asia data
66 streams. The inputs (e.g., precipitation) and resulting hydrologic estimates (a) provide a 40+ year
67 historical record for contextualizing estimates in terms of departures from average (i.e., anomalies),
68 (b) are low latency (< 1-month) for timely decision support, and (c) are familiar to the food and
69 water security user-community.

70
71 The purpose of this data descriptor is four-fold:

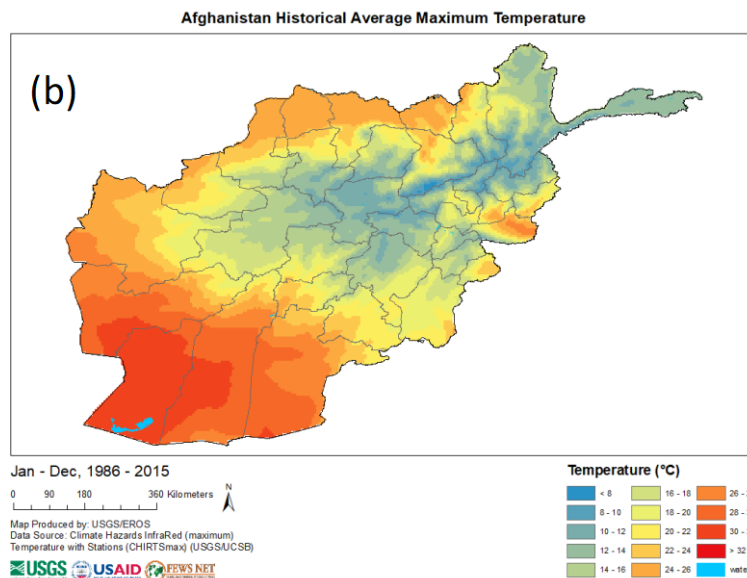
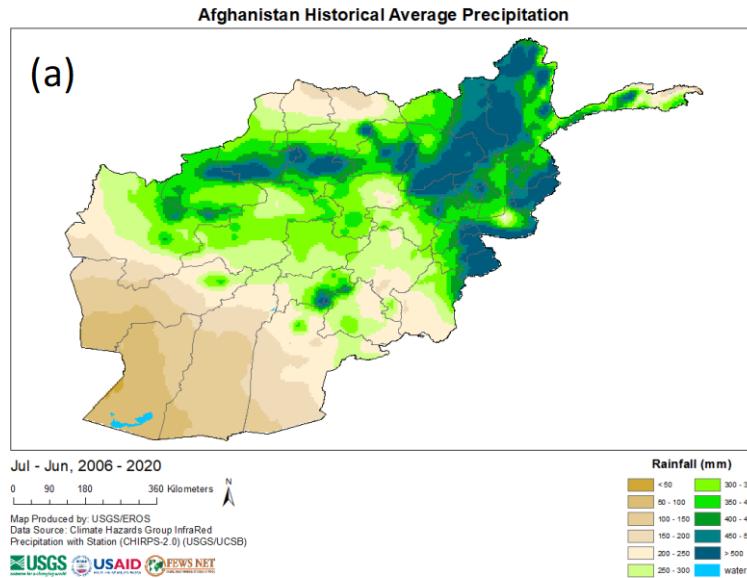
- 72 • to describe the development of the moderate resolution, low latency FLDAS hydrologic
73 monitoring system for Central Asia, specifically Afghanistan
- 74 • to increase awareness of these data resources, which are intended to be a public good,
- 75 • to demonstrate how our methods inform critical investigations that ultimately improve
76 general understanding of water resources in this important region of the world, and
- 77 • to describe a ‘convergence of evidence’ approach to hydrologic monitoring in locations
78 where all sources of information contain some level of uncertainty.

79
80 An outline of this data descriptor is as follows. Section 1.1 provides background on Afghanistan
81 Weather and Climate. Section 1.2 reviews previous studies that have conducted evaluations of the
82 meteorological inputs and hydrologic outputs of Land Data Assimilation Systems in the Central
83 Asia region. Section 2 (Methods) describes the hydrologic modeling system, parameters and
84 meteorological inputs, and model outputs. Section 3 (Results) presents comparisons of precipitation
85 inputs, and comparisons of modeled snow estimates to remotely sensed snow observations. Finally,
86 Section 4 describes an application of these data to the Afghanistan drought of 2018.

87 **1.1 Afghanistan Weather and Climate**

88 Central Asia, a region that includes Afghanistan, is water-scarce, receiving roughly 75% of its
89 annual precipitation during November–April (Oki and Kanae, 2006). In Afghanistan, rainfall is
90 highest in the northeast Hindu Kush Mountains and decreases toward the arid southwest Registan
91 Desert (Fig. 1a). Temperature follows a similar pattern with cooler temperatures in the high
92 elevation, wetter northeast, and warmer temperatures in the south and southwest (Fig. 1b). Regional
93 precipitation is strongly influenced by the El Niño-Southern Oscillation (ENSO). La Niña
94 conditions are associated with below average precipitation (FEWS NET, 2020b) and El Niño
95 conditions are associated with above average precipitation (Barlow et al., 2016; Hoell et al., 2017;
96 Rana et al., 2018; Hoell et al., 2018, 2020; FEWS NET, 2020a). Other factors with an important

97 influence on precipitation include orography, storm tracks, and the Madden–Julian oscillation
 98 (Barlow et al., 2005; Nazemosadat and Ghaedamini, 2010; Hoell et al., 2018). The last several years
 99 have experienced several ENSO events, with recent La Niña events in 2016-17, 2017-18, and 2020-
 100 2022 (NOAA CPC ENSO Cold & Warm Episodes by Season, 2021) that corresponded to droughts
 101 (FEWS NET, 2017b, 2018c, 2021).
 102



104 Figure 1. (a) Average annual precipitation in Afghanistan from 1991-2020, with overlaid province
105 boundaries. (b) Average maximum monthly temperature from (1986-2015), overlaid with province
106 boundaries. Map source USGS Knowledge Base (USGS Knowledge Base, 2021).

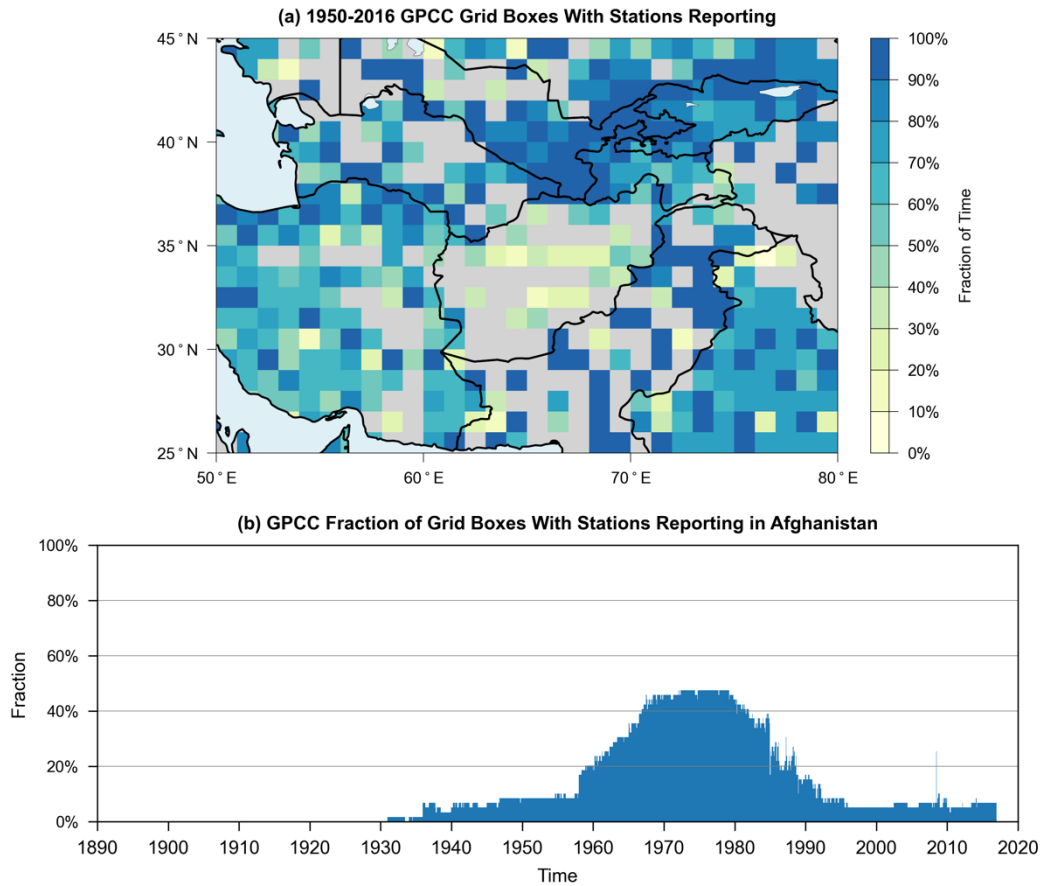
107
108 Despite Afghanistan's semi-arid climate, agriculture is an important sector, contributing 23% of its
109 gross domestic product and employing 44% of the national labor force (CIA World Factbook). High
110 mountain snowpack and snowmelt runoff are important for agricultural water supply. According to
111 FEWS NET (2018b) snowmelt runoff is responsible for "providing over 80% of irrigation water
112 used. The timing and duration of the snowmelt is a key factor in determining the volume of
113 irrigation water and the length of time that it is available, as well as its availability for use in
114 marginal areas that experience [variable] rainfall." Therefore, routine hydrologic monitoring, with a
115 particular emphasis on snow, is critical for tracking agricultural conditions and provides early
116 warning for food insecurity.

117 **1.2 Hydrologic Data Availability and Uncertainty**

118 Remote sensing and models are important inputs to climate services (Qamer et al., 2019). In the
119 Central Asia region, and especially Afghanistan estimates of meteorological inputs, and model
120 parameters have considerable uncertainty due to sparse in situ environmental observations. To
121 address these challenges, the NASA High Mountain Asia project (<https://www.himat.org/>) has
122 broadly aimed to explore the driving changes in hydrology as well as model validation and data
123 assimilation, and water budget processes from the Himalayas in the south and east to the Hindu
124 Kush in the west. These efforts and other studies of satellite derived rainfall informed the
125 configuration and interpretation of the FLDAS Central Asia and global data streams.

126
127 The primary challenge to producing and evaluating hydrologic estimates is that sparse in situ
128 precipitation observations lead to uncertainty in gridded, satellite-based precipitation estimates.
129 Precipitation station observations are used for (a) bias correction of satellite estimates and (b)
130 validation of gridded products. In terms of gridded dataset development, Hoell et al. (2015) describe
131 how lack of station observations and complex topography in Afghanistan, Iraq, and Pakistan makes
132 this issue particularly problematic. Barlow et al. (2016) also highlight the station availability across
133 the region and how that influences uncertainties in the Global Precipitation Climatology Center
134 (GPCC) version 6 (Schneider et al., 2017) dataset over Central Asia (Fig. 2a) and specifically
135 Afghanistan over time (Fig. 2b).

136



137
 138 Figure 2. (a) Station data availability underlying the GPCC version 6 dataset, for the 1950–2016
 139 period, on the 0.5°-resolution grid over Central Asia. (b) Fraction of gridcells with number of
 140 stations used as input to the GPCC rainfall dataset in Afghanistan from 1932-2016.
 141

142 In the absence of abundant in situ observations, one approach for remote sensing and model
 143 evaluation is to compare multiple input datasets and evaluate the water balance. Independent
 144 observations from the different components of the water balance (e.g., evapotranspiration, soil
 145 moisture, streamflow) help constrain estimates. We provide some background here and refer readers
 146 and data users to literature from the NASA High Mountain Asia project, specifically Yoon et al.
 147 (2019) and Ghatak et al. (2018), who explored similar configurations to the FLDAS system. This
 148 background allows the reader to appreciate the uncertainties in inputs, outputs and derived products
 149 and climate services over Afghanistan and the broader Central Asia region.
 150

151 Meteorological forcing is known to be the primary source of uncertainty in land surface model
 152 simulations (Kato and Rodell, 2007). Thus, its evaluation is important to understand the quality of
 153 model inputs and outputs. For this reason, Ghatak et al. (2018) compare four unique precipitation
 154 data sources: daily Climate Hazards center Infrared Precipitation with Stations (CHIRPS) (Funk et

155 al., 2015), NOAA’s Global Data Assimilation System (GDAS) (Derber et al., 1991), and two
156 estimates from NASA’s Modern Era Reanalysis for Research and Applications version 2 (MERRA-
157 2) (Gelaro et al., 2017). They find that annual CHIRPS and GDAS precipitation estimates had
158 similar bias and root mean squared error over Afghanistan with respect to APHRODITE (Asian
159 Precipitation Highly Resolved Observational Data Integration Toward Evaluation) rain-gauge
160 derived product (Yatagai et al., 2012). CHIRPS had a higher correlation with APHRODITE. Ghatak
161 et al. (2018) further evaluated the quality of rainfall inputs based on the performance of
162 evapotranspiration and other derived outputs. The authors caution that gridded precipitation
163 estimates that have in situ inputs, like CHIRPS, may systematically underestimate precipitation in
164 mountainous regions. We keep this consideration in mind when interpreting differences between
165 FLDAS global and Central Asia data streams.

166
167 Yoon et al. (2019) compare precipitation estimates from 10 different products including
168 APHRODITE, CHIRPS, GDAS, and MERRA-2, across a broad region of High Asia, including a
169 portion of Afghanistan. They find that all datasets generally capture the spatial pattern of rainfall
170 and that the products tend to agree more at high elevations, where it is unlikely there are station
171 observations. Like Ghatak et al. (2018), they found CHIRPS and APHRODITE to have a lower
172 average precipitation than GDAS, attributable to the incorporation of sparse gauge data.

173
174 In addition to precipitation, other meteorological inputs are important for accurate hydrologic
175 estimates. Yoon et al. (2019) conducted an intercomparison of near surface air temperature
176 estimates from three model analysis products (European Centre for Medium-Range Weather
177 Forecasts (ECMWF; Molteni et al., 1996), GDAS, and MERRA-2). They noted a statistically
178 significant upward trends in GDAS and ECMWF temperature, as well as consistently higher
179 temperatures in MERRA-2. We see the same pattern when averaging across Afghanistan. Yoon et
180 al. (2019) conclude that improvements in the meteorological boundary conditions would be needed
181 to reduce the uncertainty in the terrestrial budget estimates. These sentiments are echoed in Qamer
182 et al. (2019).

183
184 Despite known uncertainties, Schiemann et al. (2008) find that gridded precipitation estimates can
185 qualitatively identify large scale spatial distribution of precipitation, seasonal cycles, and interannual
186 variability (i.e., wet and dry years) across Central Asia. Long-term estimates of rainfall from
187 satellite derived products, as well as derived historical time series from hydrologic modeling, can be
188 used as a baseline of “observations,” from which we can have a sense of relative conditions, i.e.,
189 anomalies and variability. When this historical record is harmonized with a routine monitoring
190 system, current conditions can be placed in historical context. Anomaly-based representation of
191 hydrologic extremes can provide confidence in modeled estimates that have the potential to
192 influence agricultural, water resources and food security outcomes. For these reasons one of the
193 requirements for FLDAS input is that there is a sufficiently long historical record for
194 contextualizing estimates in terms of anomalies.

195

196 From a climate services perspective, the reliance on the representation of relatively wet and dry
197 conditions, as well as a “convergence of evidence” approach, provide useable information despite
198 the above-mentioned uncertainties. A convergence of evidence approach that draws on (quasi-
199 independent sources of information is useful to understand actual conditions. For convergence of
200 Earth observations, hydrologic models can generate ensembles of historical, current, or future
201 estimates of snow, streamflow, soil moisture, and evapotranspiration, which can then be compared
202 to satellite derived estimates of surface water (e.g., McNally et al., 2019), soil moisture (e.g.,
203 McNally et al., 2016), vegetation conditions and evapotranspiration (e.g., Jung et al., 2019; Pervez
204 et al., 2021), snow cover (e.g., Arsenault et al., 2014), in situ streamflow (e.g. Jung et al., 2017) and
205 others. Hydrologic estimates can also be compared to outcomes in crop production (e.g., (e.g.,
206 McNally et al., 2015; Davenport et al., 2019; Shukla et al., 2020), and nutrition, health, and food
207 security (e.g., Grace and Davenport, 2021) to provide a qualitative understanding of both hydrologic
208 model performance and conditions on the ground. In this paper we provide an example for 2018
209 where drought conditions were associated with crisis levels of acute food insecurity over most of
210 Afghanistan (FEWS NET, 2018c).

211
212 To summarize, our experience and the literature have characterized uncertainties in available
213 meteorological forcing for the region. GDAS, CHIRPS, and MERRA-2 were chosen for the FLDAS
214 system based on our project requirements of (a) a sufficiently long historical record for
215 contextualizing estimates in terms of anomalies (b) low latency (< 1-month) for timely decision
216 support, (c) familiar to the FEWS NET user-community, and (d) prior evaluation by our team and
217 the broader community. We note here and describe in more detail later that the Integrated Multi-
218 satellite Retrievals for the Global Precipitation Mission (IMERG), a NASA precipitation product
219 (Huffman et al., 2020) also meets these requirements, since version 6 which was released in 2019
220 (after these studies and initial FLDAS configuration). We will a describe IMERG, GDAS, and
221 MERRA-2 comparison in the Results (Section 3).

222 **2 Methods**

223 **2.1 Land Surface Modeling System & Parameters**

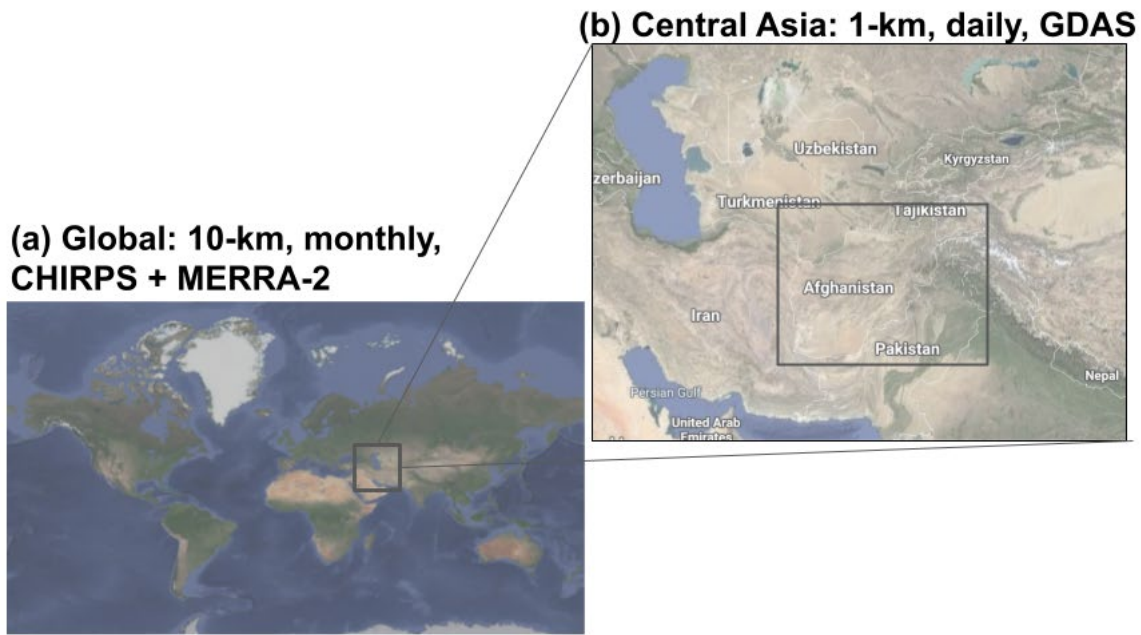
224 A land surface model (LSM) can provide spatially and temporally continuous information about the
225 water and energy budgets of the land surface. This information is useful for food and water security
226 applications in places where in situ measurements of rainfall, soil moisture, snow and runoff are
227 sparse. This is particularly relevant in mountainous places like Afghanistan where heterogeneous
228 geography limits the representativeness of sparse in situ measurements. The FLDAS (McNally et
229 al., 2017) utilizes the NASA’s Land Information System Framework (LISF), which is composed of
230 a pre-processor, the Land surface Data Toolkit (LDT) (Arsenault et al., 2018), the Land Information
231 System (Kumar et al., 2006; Peters-Lidard et al., 2007), and the Land Verification Toolkit (Kumar
232 et al., 2012). In this data descriptor we describe the two configurations of the FLDAS data streams
233 used for Central Asia food and water security applications. It uses the Noah 3.6 LSM (Chen et al.,

234 1996; Ek et al., 2003) for the two data streams (Fig. 3 and Table 1). The first data stream is global,
235 at ~1 month latency, and provides monthly average outputs on a 10-km grid from 1982-present. The
236 second data stream centered on Central Asia, ~1 day latency, provides daily average outputs at 1-km
237 from 2001-present.

238
239 One important feature, added by the NASA LISF software development team, is the radiation
240 correction described in Kumar et al. (2013), which improves the representation of snow dynamics
241 with respect to slope and aspect corrections on the downward solar radiation field. Another
242 noteworthy feature is the method of the Central Asia data stream restart (i.e., annual initialization
243 based on climatology), which was developed to address an issue of excessive inter-annual snow
244 accumulation found in the Noah LSM. First, a nine-year spin-up of the system was performed to
245 produce stable snow and soil moisture conditions. Next, the resulting model states were compared
246 with the Moderate Resolution Imaging Spectroradiometer (MODIS) Maximum Snow Extent data
247 originally computed by NOAA National Operational Hydrologic Remote Sensing Center (Greg Fall,
248 NOAA Operational Data Center, written communication., 2014). Then, the model-estimated
249 conditions were adjusted to produce a climatological model state for 1 October that is used to
250 initialize each year. This approach ensures that the ‘water year,’ beginning 1 October, is initialized
251 with a reasonable initial amount of snowpack. While this method does effectively manage excessive
252 inter-annual modeled snow accumulation, the user should be aware that using the climatological
253 model state will persist for ~1-2 months in the water and energy balance of the LSM until they are
254 superseded by “observed” meteorological inputs for the current water year. Preliminary work
255 indicates that this issue will be resolved in future updates. In contrast, the global data stream does
256 not use this 1 October initialization procedure.

257 Although the two data stream specifications are largely the same, there are some differences related
258 to the input forcings, parameters and specifications (Table 1) and model spin-up procedures.

259



260
 261 Figure 3. The FEWS NET Land Data Assimilation System (FLDAS) domains for (a) the global data
 262 stream at 10-km spatial resolution and ~1 month latency for monthly averaged hydrologic estimates
 263 and (b) the Central Asia data stream at 1-km spatial resolution and ~1 day latency for daily averaged
 264 hydrologic estimates. Imagery 2021 TerraMetrics, Map data © Google.

265
 266
 267 Table 1. FEWS NET Land Data Assimilation System (FLDAS) specifications for (A) global data
 268 stream, 10-km monthly with CHIRPS+MERRA-2; and (B) Central Asia data stream, 1-km, daily
 269 with GDAS.

	Global	Central Asia
Spatial Extent	179.95°W- 179.95°E, 59.95°S-89.95°N	30-100°E, 21-56°N
Landmask	Generated from MODIS using LISF-LDT, with MOD44w mask applied post-processing.	MOD44w (Carroll et al., 2017)
Landcover	IGBP landcover	IGBP landcover
Elevation	Shuttle Radar Topography Mission SRTM (NASA JPL, 2013)	SRTM

Albedo	National Centers for Environmental Prediction (NCEP) albedo (Csiszar and Gutman, 1999) & MODIS-based Max Snow Albedo (Barlage et al., 2005)	NCEP albedo & MODIS-based Max Snow Albedo
Vegetation Parameters	NCEP greenness fraction (Gutman and Ignatov, 1998)	NCEP greenness fraction
Non-Precipitation Meteorological Inputs	MERRA-2	GDAS
Soil Texture	Food and Agricultural Organization (FAO) soil texture & properties (Reynolds et al., 2000)	FAO soil texture & properties
Precipitation Inputs	CHIRPS daily precipitation, downscaled to 6-hourly with LDT	GDAS 3-hourly precipitation
Specifications	Noah 3.6.1	Noah 3.6.1
Map Projection	Geographic Latitude-Longitude	Geographic Latitude-Longitude
Software Version	7.2	7.3
Spatial Resolution	10-km	1-km
Temporal Coverage	1982-01-01 to present	2000-10-01 to present
Model Timestep	15-min timestep	30-min timestep
Met. Forcing Heights	2-m Air Temperature (Tair), 10-m Wind	2-m Tair, 10-m Wind
Soil layers (meters)	0-0.1; 0.1-0.4; 0.4-1.0; 1-2	0-0.1; 0.1-0.4; 0.4-1.0; 1-2
Features	radiation correction	radiation correction

270

271 The parameters and specifications listed in Table 1 are largely default settings defined by the Noah
272 LSM community (NCAR Research Applications Library, 2021). Ongoing research aims to identify
273 where model output performance can be improved with parameter updates. Evaluating parameter
274 updates had similar challenges as evaluating input forcing described in Section 1.2: without reliable
275 reference data it is difficult to determine a “best” input. For example, we have explored changing
276 soil parameters from FAO to International Soil Reference and Information Centre (ISRIC) SoilGrids
277 database (Hengl et al., 2017). This change did not result in improvements in streamflow statistics in
278 southern Africa, nor in soil moisture anomalies’ ability to represent drought events. We expect
279 similar results in Afghanistan where, e.g., streamflow will be sensitive to a change in soil

280 parameters and the lack of referenced data to evaluate if there is an improvement. Moreover, our
281 model runs at 0.1 and 0.01 degrees may not fully exploit the added value of the 250m soil grids as
282 noted in Ellenburg et al. (2021) for a LISF application in East Africa.

283 Vegetation parameters are also potential sources of improvement whose importance to LDAS
284 hydrologic estimates has been highlighted (e.g., Miller et al., 2006). We have found the NCEP
285 estimates of green vegetation fraction (GVF) to be sufficient for this configuration of Noah 3.6. We
286 found that a time series of GVF derived from the Normalized Difference Vegetation Index (NDVI)
287 did not improve representation of droughts in eastern Africa. However, future FLDAS global and
288 Central Asia versions can be run with Noah-Multi parameterization (Noah-MP) (Niu et al., 2011)
289 which has multiple vegetation options and relies on either Leaf Area Index rather or GVF. This
290 model update is expected to open possibilities for choice of datasets to meet our application needs
291 and potentially improve representation of the water balance.

292 **2.2 Meteorological Forcing Inputs**

293 As previously discussed, precipitation is a critical input to land surface models. The lower-latency
294 Central Asia data stream is a daily product, forced with GDAS (Derber et al., 1991) 3-hourly
295 precipitation, which is available from 2001 to present at <1-day latency. This dataset was chosen
296 because of its latency. The global data stream is driven by the daily CHIRPS product (Funk et al.,
297 2015), which is available from 1981 to present at ~ 5-day latency for CHIRPS Preliminary and ~1.5-
298 month latency for CHIRPS Final. The CHIRPS products were chosen as inputs because of their
299 proven performance in the literature, which has made it the “gold standard” for food and water
300 security monitoring by organizations like FEWS NET, the World Food Program, and others who
301 need up-to-date estimates and a 40+ year historical record. As mentioned earlier, lack of rainfall
302 stations for bias correction of satellite-derived estimates and evaluation poses a major challenge.
303 However, we find that the GDAS rainfall product and the CHIRPS rainfall product are adequate for
304 routine monitoring and, along with additional sources of remote sensed information, are important
305 for convergence of evidence when making a best estimate at land surface states and fluxes.

306
307 Before the daily CHIRPS rainfall data can be used as input to the FLDAS models, the daily
308 precipitation is pre-processed to a sub-daily timestep, using the LDT component of the LISF
309 software. LDT temporally disaggregates the daily CHIRPS rainfall using an approach similar to the
310 North American LDAS precipitation temporal downscaling (Cosgrove et al., 2003). For this
311 approach, we use a finer timescale MERRA-2 precipitation timescale as a reference dataset to
312 represent an accurate diurnal cycle. We note that this step in our methodology facilitates the solving
313 of FLDAS water and energy balances at a sub-daily timestep. However, for Central Asia we do not
314 have sufficient reference data available to assess the importance of sub-daily precipitation
315 distribution, as was demonstrated by Sarmiento et al. (2021) for the United States where adequate
316 reference data are available. For spatial downscaling, coarser scale meteorological forcings are
317 spatially disaggregated to the output resolution (0.01, and 0.1 degree for Central Asia and global,
318 respectively) in the LISF using bilinear interpolation.

319 The FLDAS models require additional meteorological inputs, including air temperature, humidity,
320 radiation, and wind. The lower-latency Central Asia data stream uses GDAS 3-hourly
321 meteorological inputs available from 2001-present at <1-day latency. For a longer historical record,
322 the global data stream uses MERRA-2 (Gelaro et al., 2017) (1979-present) 1-hourly products with a
323 two-week latency. Over the Afghanistan domain GDAS temperature has an upward trend, whereas
324 MERRA-2 is consistently warmer before 2010. We find that GDAS and MERRA-2 temperature
325 estimates are of similar magnitude during 2011-2020. Similar results were noted by Yoon et al.
326 (2019) who found an upward trend in GDAS temperature, as well as consistently higher
327 temperatures in MERRA-2 across a broad High Asia domain.

328 **2.3 Model Evaluation Statistics and Comparison Data**

329 In addition to guidance from previous studies (Section 1.2), we assessed the quality of our modeling
330 outputs by conducting comparisons between (1) FLDAS satellite rainfall inputs and other satellite
331 precipitation estimates, and (2) model estimated snow cover fraction and satellite derived snow
332 cover fraction estimates.

333
334 For the precipitation analysis, we compare CHIRPS and GDAS inputs to the Integrated Multi-
335 satellite Retrievals for the Global Precipitation Mission (IMERG), a NASA precipitation product
336 that integrates passive microwave and infrared satellite data with surface station observations
337 (Huffman et al., 2020). The IMERG Final Run precipitation product, available at ~ 2-month latency
338 (thus not suitable for our monitoring applications) has been used in numerous verification studies,
339 including studies over Africa (Dezfuli et al., 2017), South America (Gadelha et al., 2019; Manz et
340 al., 2017), and the mid-Atlantic region of the United States (Tan et al., 2016). These studies
341 demonstrated that IMERG Final Run was able to capture large spatial patterns and seasonal and
342 interannual patterns of rainfall. However, fewer studies have explored the performance of the lower
343 latency IMERG Late Run (doi: 10.5067/GPM/IMERGDL/DAY/06) product that we use here.
344 Kirshbaum et al. (2016) include a qualitative comparison for CHIRPS Final and IMERG Late Run
345 for the Southern Africa start-of-season 2015. IMERG Late Run appears to perform similarly to the
346 1.5-month latency CHIRPS Final and outperform the 1-day latency NOAA Rainfall Estimate
347 version 2 (RFE2) product (Xie and Arkin, 1996). Differences in the daily rainfall distribution
348 patterns between IMERG Final Run and CHIRPS Final have also been shown to affect the resulting
349 hydrological modeled output in simulations done using the NASA LISF (Sarmiento et al., 2021).

350
351 For the snow cover fraction (SCF) analysis, we compare the global and Central Asia data streams
352 with the MODIS daily SCF product, MOD10A1 Collection 6 (Hall and Riggs, 2016). MOD10A1
353 data are available at 500-m spatial resolution from February 2000 to the present. SCF is generated
354 using the Normalized Difference Snow Index (NDSI) and additional filters to reduce error and flag
355 uncertainty. Routine qualitative comparisons, which can be viewed on the NASA LISF FEWS NET
356 project website, generally show agreement between the model and MODIS SCF, as well as
357 occurrence of cloud cover (<https://ldas.gsfc.nasa.gov/fldas/models/central-asia>). Following
358 Arsenault et al. (2014), we aggregated pixels to 0.01 degree to reduce error related to sensor viewing

359 angles and gridding artifacts. For this analysis, using MODIS SCF as “truth,” we determined True
360 Positives (TP), True Negatives (TN), False Negatives (FN) and False Positives (FP). We then
361 computed probability of detection (POD) where $POD = (TP / (TP + FN))$ and False Alarm Rate
362 (FAR) where $FAR = (FP / (FP + TN))$. We computed these for the total area of Afghanistan (60-76E,
363 28-39N), as well as by basin (Fig. 4). This paper does not compare modeled snow water equivalent
364 (SWE) to independent snow observations because, as noted by Yoon et al. (2019), direct evaluation
365 of snow mass and SWE) is difficult over Central Asia due to poor coverage of accurate snow
366 observations. We follow the Yoon et al. (2019) recommendation to conduct quantitative SCF
367 comparisons and provide qualitative SWE analysis in Applications, Section 4.

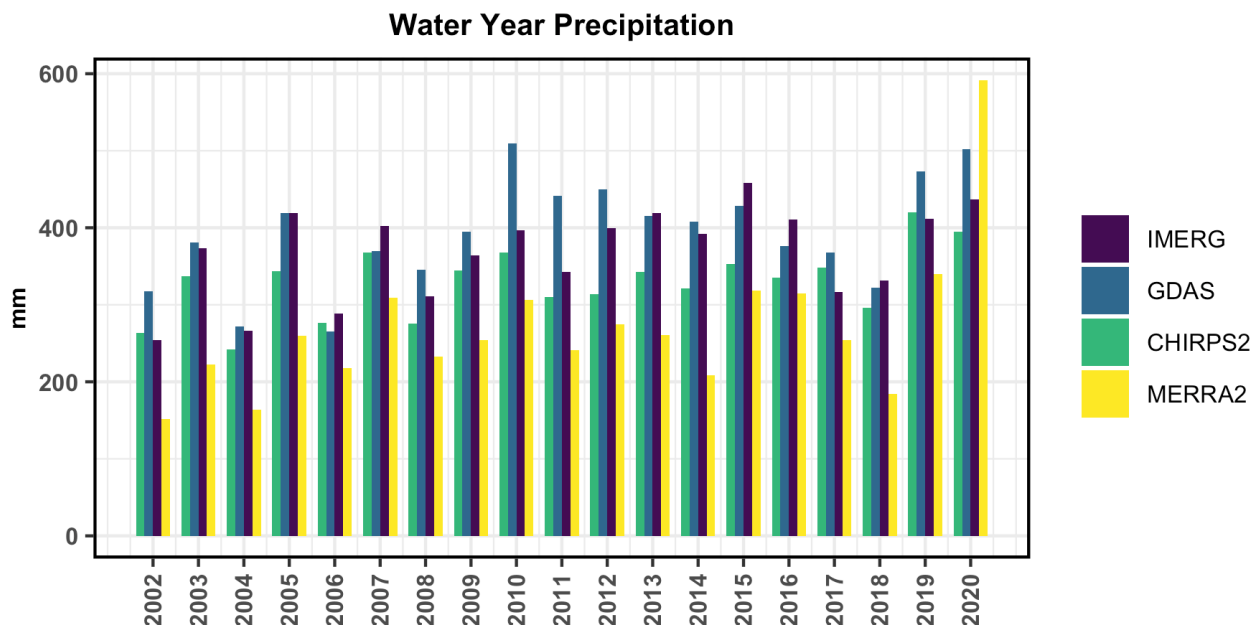
368
369 In addition to rainfall and snow comparisons, we conducted monthly pixel-wise comparison of
370 Central Asia and the global run’s estimates of evapotranspiration (ET) and soil moisture versus
371 Operational Simplified Surface Energy Balance (SSEBop, (Senay et al., 2013)). ET and Soil
372 Moisture Active Passive (SMAP) Level 3 (Entekhabi et al., 2010, 2016) using the Normalized
373 Information Contribution (NIC) metric following Sarmiento et al., (2021). The analysis was
374 performed for the period 2016-2021 to match the SMAP record. The NIC metric first computes
375 anomaly correlations between the model runs and the reference dataset and then computes the
376 difference between the performance of each model run using a scale of -1 to +1 to highlight if the
377 global or Central Asia data stream performs better with respect to the reference. To make the
378 comparisons, the reference datasets (SMAP and SSEBop) were re-gridded to match the grid spacing
379 and locations of the experiment model outputs.

380 **3 Results**

381 **3.1 Gridded Rainfall Comparison**

382 We have two data streams for Central Asia applications with different precipitation inputs: 1) the
383 global data stream with CHIRPS precipitation at 10-km spatial resolution provides a long-term
384 consistent data record; and 2) the Central Asia data stream with GDAS precipitation at 1-km
385 provides near real time, finer spatial resolution updates. These two data streams have their
386 respective errors and allow data users to apply a convergence of evidence approach for food and
387 water security applications. This section presents a comparison of the GDAS, and CHIRPS
388 precipitation inputs used for the Central Asia and global data streams, respectively. We also include
389 IMERG Late Run for comparison as a high quality, low latency product. Future work may
390 incorporate the IMERG Late Run precipitation inputs into FLDAS simulations. We also include
391 MERRA-2 precipitation for comparison. Pair-wise correlations are shown in Table 2. CHIRPS
392 Final, IMERG Late Run and GDAS ($R \geq 0.90$) are well correlated in terms of average daily
393 precipitation (mm/day) at the monthly and annual (i.e., water year) timestep. MERRA-2 correlations
394 with these datasets are lower at the monthly ($0.75 \leq R \leq 0.81$) and water year ($0.64 \leq R \leq 0.69$)
395 timesteps. Fig. 4 shows the time series of the precipitation products for their overlapping period of
396 record (2001-2020), which illustrates how they vary in time, and shows some general patterns in
397 terms of relative precipitation in mm: GDAS (blue) and IMERG Late Run (purple) tend to have the

398 highest precipitation totals, CHIRPS (green) has lower precipitation but is higher than MERRA-2
 399 (yellow) which tends to have the lowest precipitation, until 2019 when it is notably higher than the
 400 other products.



401
402

403 Figure 4. Afghanistan water year precipitation for CHIRPS, GDAS, IMERG Late Run, and
 404 MERRA-2.

405
406
407

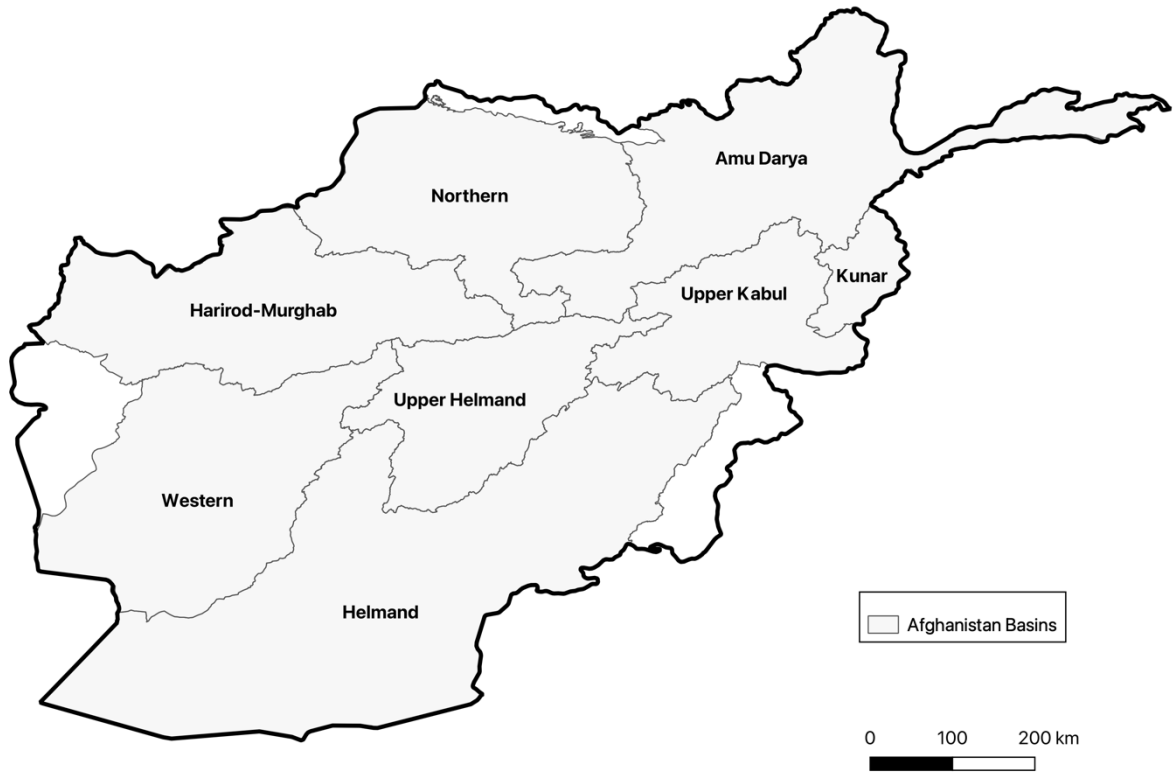
406 Table 2. Afghanistan spatial average Spearman Rank Correlation (R) of monthly (water year)
 407 precipitation 2001-2020

	GDAS	CHIRPS Final	IMERG Late Run
GDAS	x	-	-
CHIRPS Final	0.91 (0.92)	x	-
IMERG Late Run	0.91 (0.89)	0.92 (0.90)	x
MERRA-2	0.75 (0.64)	0.78 (0.68)	0.81(0.69)

408

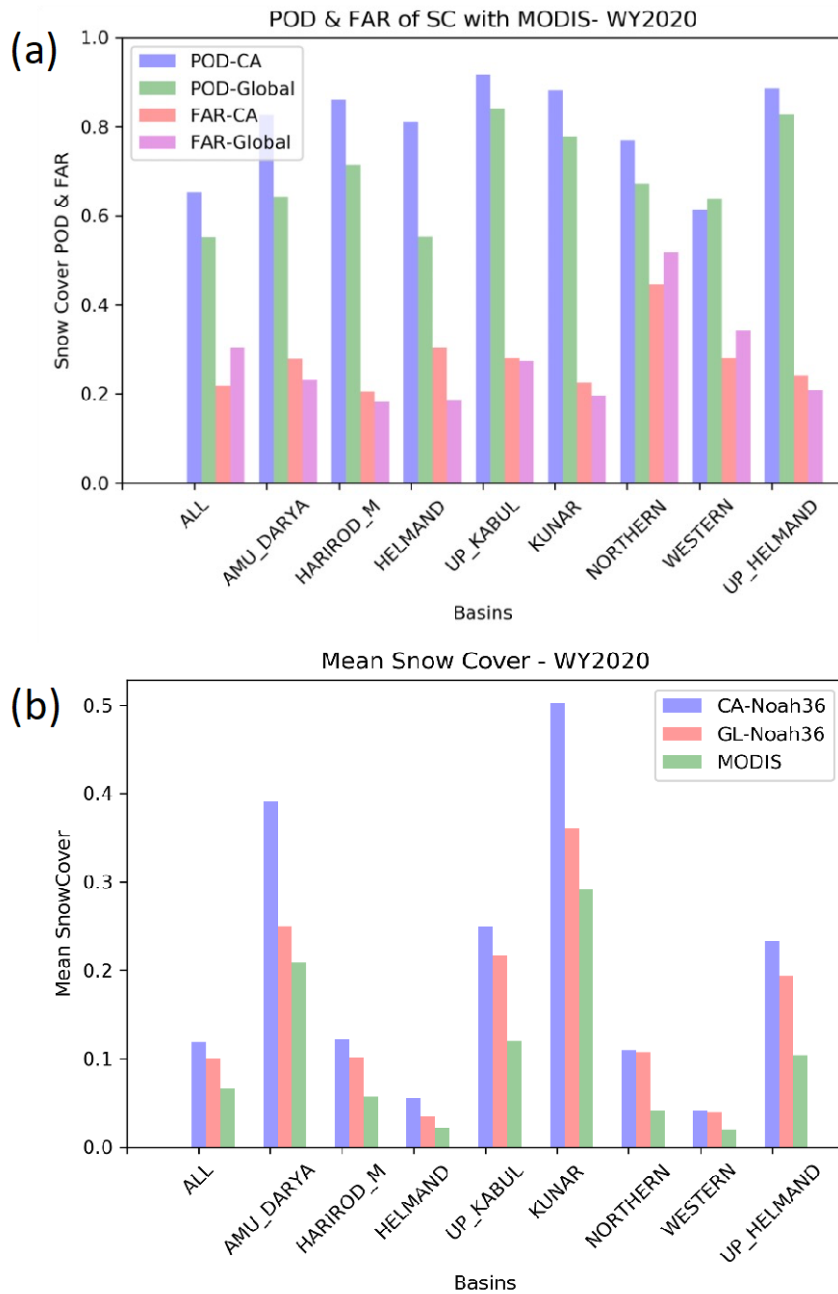
409 3.2 Remotely Sensed and Modeled Snow comparisons

410 The estimation of snow is important for Afghanistan and Central Asia because it is a critical
 411 contributor to water resources and irrigated agriculture. We compared average SCF (Fig. 6a), POD,
 412 and FAR statistics (Fig. 6b) relative to MODIS SCF over eight hydrologic basins in Afghanistan.
 413



414
415
416

Figure 5. Hydrologic basins used in the analysis of categorical statistics for snow covered fraction.



417
 418 Figure 6. (a) Mean snow cover fraction for the entire area and by hydrologic basin for MODIS
 419 Snow Cover Fraction (SCF), Central Asia (CA) and global (GL) data streams for water year 2020.
 420 (b) Probability of Detection (POD) of snow presence, and False Alarm Rate (FAR) for the Central
 421 Asia (CA) and global data streams relative to the MODIS SCF for water year 2020.
 422

423 Overall, both model runs estimate greater average SCF than the MODIS SCF product. The Central
424 Asia data stream has consistently higher average snow cover for all basins compared to MODIS
425 SCF estimates and the global data stream. Perhaps not surprisingly that the Central Asia data stream
426 performs consistently better in POD (by basin = ~80%) except for the Western Basin. Similarly, the
427 FAR of the Central Asia data stream is higher where POD is higher except for the Northern Basin.
428 The difference in statistics may be related to the different forcing inputs or the higher spatial
429 resolution of the Central Asia data stream. Kumar et al. (2013) note that higher spatial resolution
430 was important for snow dominated basins.

431
432 In addition to precipitation and snow cover comparisons we conducted comparisons with remotely
433 sensed soil moisture and ET (not shown). We found that in general, GDAS derived estimates of ET
434 consistently performed better over Afghanistan in terms of pixel-wise anomaly correlation and NIC
435 with SSEBop ET. Meanwhile, neither modeled estimate of soil moisture consistently outperformed
436 the other with respect to SMAP. The ET results lend some support to the quality of the Central Asia
437 data stream estimates. However, the lack of signal in the soil moisture comparisons suggests that
438 more careful analysis of the model and remote sensing errors is required before drawing conclusions
439 regarding which data stream is “best.”

440 **3.3 Discussion of results compared to previous studies**

441 Despite the lack of ground-based observations, our analysis shows that the remotely sensed
442 estimates and the models have good correspondence with other sources of evidence in terms of
443 seasonal timing and performance. This provides analysts with confidence when using the FLDAS
444 snow estimates, in tandem with other sources, as an input to food security assessments. Our
445 approach is supported by other studies that have explored the challenges of evaluating hydrologic
446 estimates over the region (Immerzeel et al., 2015; Ghatak et al., 2018; Yoon et al., 2019; Qamer et
447 al., 2019).

448
449 Yoon et al. (2019) show that their LSM ensembles of SCF have an average POD of 72% and FAR
450 of 36%, which is within the range of our POD and FAR statistics (60-80% POD; 20-40% FAR)
451 compared to MODIS SCF. The categorical statistics indicate that Central Asia (GDAS) tends to
452 have both a higher probability of detection and false alarm rate, indicating higher averages than
453 MODIS SCF and global (CHIRPS).

454
455 With respect to the soil moisture and ET comparisons, we found that the Central Asia data stream
456 estimates of ET were better correlated with SSEBop ET, but neither data stream was consistently
457 better correlated with SMAP. These differences could be a function of non-precipitation differences,
458 or higher spatial resolution. Ghatak et al. (2018) also found that the choice of reference dataset (with
459 its own characteristics and errors) was an important factor.

460

461 In general, given the lack of clarity on “best” FLDAS data stream, the convergence of evidence
 462 approach allows us to consult both data streams, leveraging the longer time series of CHIRPS and
 463 the lower latency of GDAS.

464 3.4 Limitations and Future Developments

465 Given the need for multiple data streams for convergence of evidence, we have summarized the pros
 466 and cons of the Central Asia and global data streams in Table 3.

467
 468 Table 3. Pros and cons of the two data streams

	Central Asia: Noah 3.6 with GDAS (2000-present)	Global: Noah 3.6 with CHIRPS+MERRA-2 (1982-present)
Pros	1-km	less computationally intensive
	1-day latency, daily timestep	longer time record
	Snow estimates available in USGS Early Warning eXplorer https://earlywarning.usgs.gov/fews/ewx/	CHIRPS & MERRA-2 forcing spatial resolution does not change over time (stable climatology)
		Water and Energy balance available in NASA GIOVANNI https://giovanni.gsfc.nasa.gov/giovanni/ ; Google Earth Engine https://developers.google.com/earth-engine/datasets/tags/fldas ; Climate Engine https://climateengine.com/
Cons	more computationally intensive	lower resolution (10-km)
	shorter time record	~30-day latency
	GDAS forcing resolution changes over time (unstable climatology) (NOAA NCEP https://www.emc.ncep.noaa.gov/gmb/STATS/html/model_changes.html)	not publicly available at daily timestep
	large data volume, difficult to move	

469

470 IMERG version 6 was released in 2019 and includes rainfall estimates processed back to 2000. Prior
 471 to this change we had found encouraging results when comparing the onset of rainy season using
 472 both IMERG Late Run and CHIRPS (Kirschbaum et al., 2016). However, at that time the period of
 473 record was a limitation for computing anomalies. We now have an adequate period of record, and
 474 IMERG Late Run is planned to be part of the upcoming FLDAS global and FLDAS Central Asia
 475 releases. We are also encouraged by the quality of IMERG at the daily timestep when compared to
 476 CHIRPS over the United States where accurate reference data are available (Sarmiento et al., 2021).
 477

478 In addition to IMERG other promising rainfall datasets are in development. Ma et al. (2020) have
 479 developed the AIMERG dataset that combines IMERG Final Run with the APHRODITE rain-gauge
 480 derived product (Yatagai et al., 2012). Another promising dataset is CHIMES (Funk et al., 2022), a
 481 blend of CHIRPS and IMERG, whose developers have been exploring the strengths and limitations
 482 of these two datasets and their fusion to produce an optimal product.
 483

484 With respect to other FLDAS developments, FLDAS global and Central Asia are planned to be
 485 transition to Noah-MP. This will allow for improved representation of snowpack and groundwater.
 486 This will also necessitate the use of different parameters, e.g., leaf area index, as well as the
 487 potential to explore different parameter sets like ISRIC soils. In the meantime, multi-forcing and
 488 multi-model ensembles, and convergence of evidence with other remotely sensed data and field
 489 reports, are a viable approach for providing hydrologic estimates for various applications.

490 **4 Applications**

491 These data from global and Central Asia data streams are routinely used in several FEWS NET
 492 information products listed in Table 4. NOAA’s Climate Prediction Center (CPC) International
 493 Desks provide a weekly briefing on the past week’s weather conditions and 1– 2-week forecasts for
 494 FEWS NET regions of interest, including Central Asia. There is also a monthly FEWS NET
 495 Seasonal Monitor and a monthly Seasonal Forecast Review for which these data provide
 496 information on the current state of the snowpack, soil moisture, and runoff. These “observed
 497 conditions" can then be qualitatively combined with forecasts 1 week to many months in the future
 498 to assess potential hydro-meteorological hazards. To demonstrate the role of these data in the early
 499 warning process, at different points in the season, we provide an example of the 2017-2018 wet
 500 season in Afghanistan during a La Niña event that contributed to drought.
 501

502 Table 4. Routine Applications of FLDAS Central Asia’s Afghanistan hydrologic data.

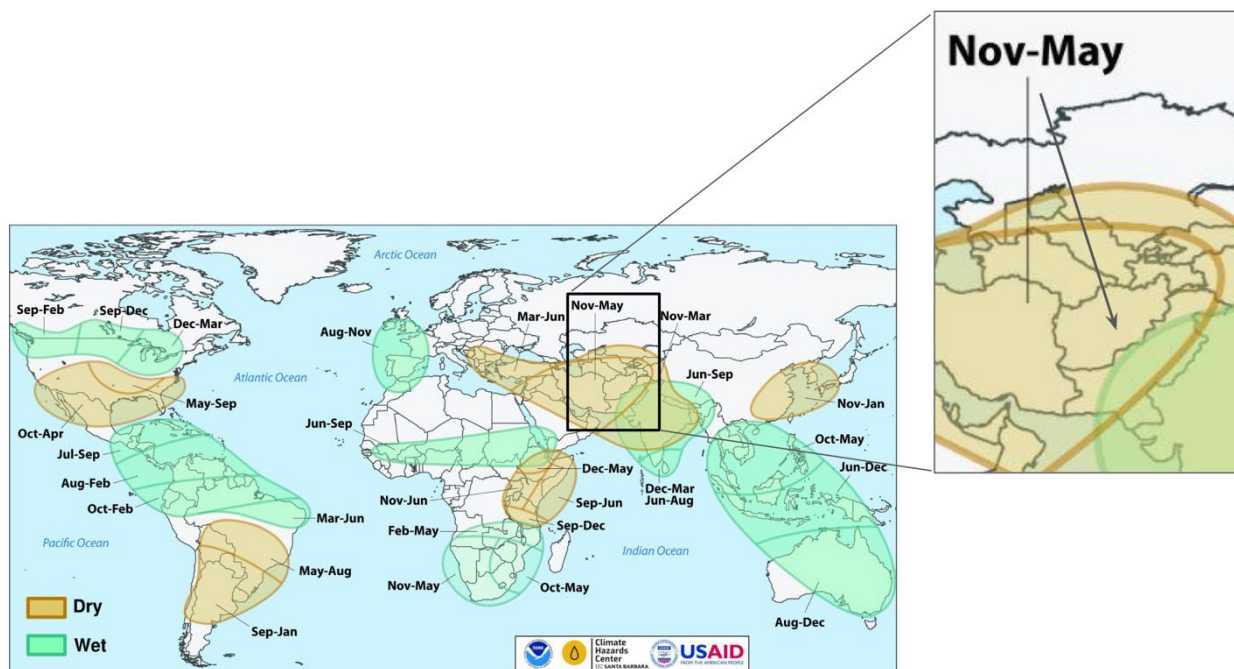
Routine application of these data	Weblink to updates	Notes
FEWS NET Global Weather Hazards	https://fews.net/global/global-weather-hazards/	shapefiles https://ftp.cpc.ncep.noaa.gov/fews/weather_hazards/

Summary produced by NOAA CPC	https://www.cpc.ncep.noaa.gov/products/international/index.shtml	
Seasonal Monitor	https://earlywarning.usgs.gov/fews/afghanistan/seasonal-monitor	Updated near the middle of each month from October - May, the wet season.
FEWS NET Food Security Outlook Brief	https://fews.net/central-asia/afghanistan	Information on snow or other hydrology included if applicable
Crop Monitor for Early Warning	https://cropmonitor.org/index.php/cmreports/early-warning-report/	Information on early warning and crop conditions

503

504 4.1 Snow Monitoring & Seasonal Outlooks

505 As previously mentioned, and as shown in Fig. 7, Afghanistan and the broader region is strongly
506 influenced by La Niña, which tends to increase the likelihood of below average precipitation.
507 Depending on this and antecedent conditions there is an increased likelihood of below average
508 snowpack, reduce springtime streamflow and flood risk, reduce summer irrigation water
509 availability, and crop yield losses.
510



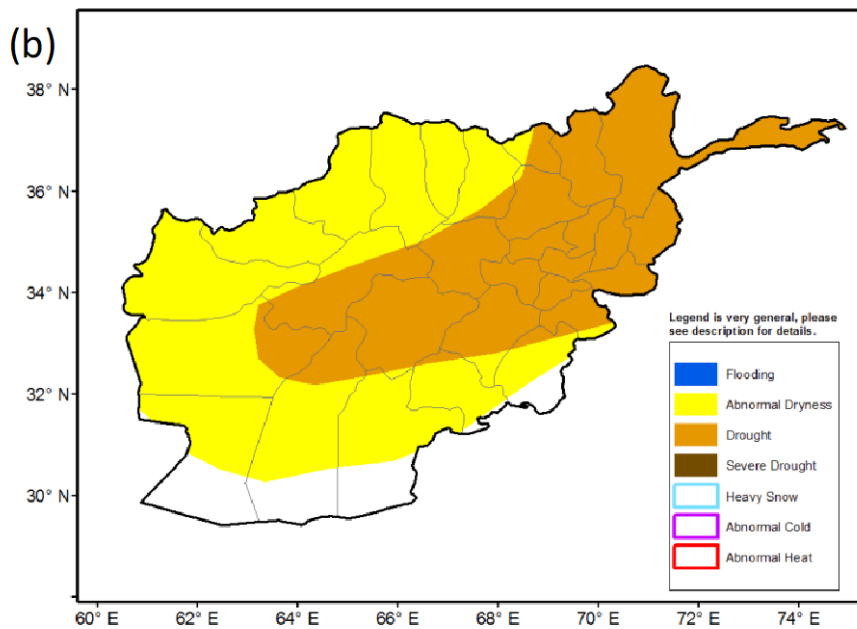
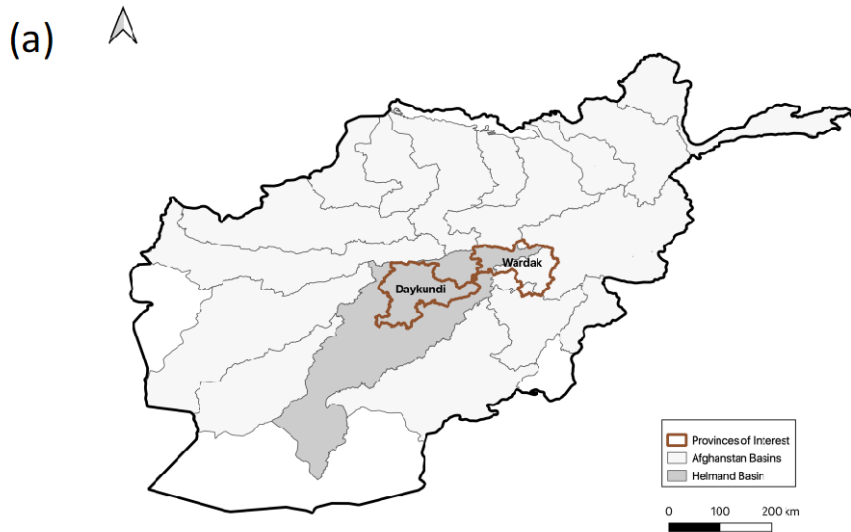
511

512 Figure 7. Timing of wet and dry conditions related to La Niña. Increased likelihood of dry
513 conditions from November-May for Afghanistan during La Niña events. Image from FEWS NET
514 (2020b).

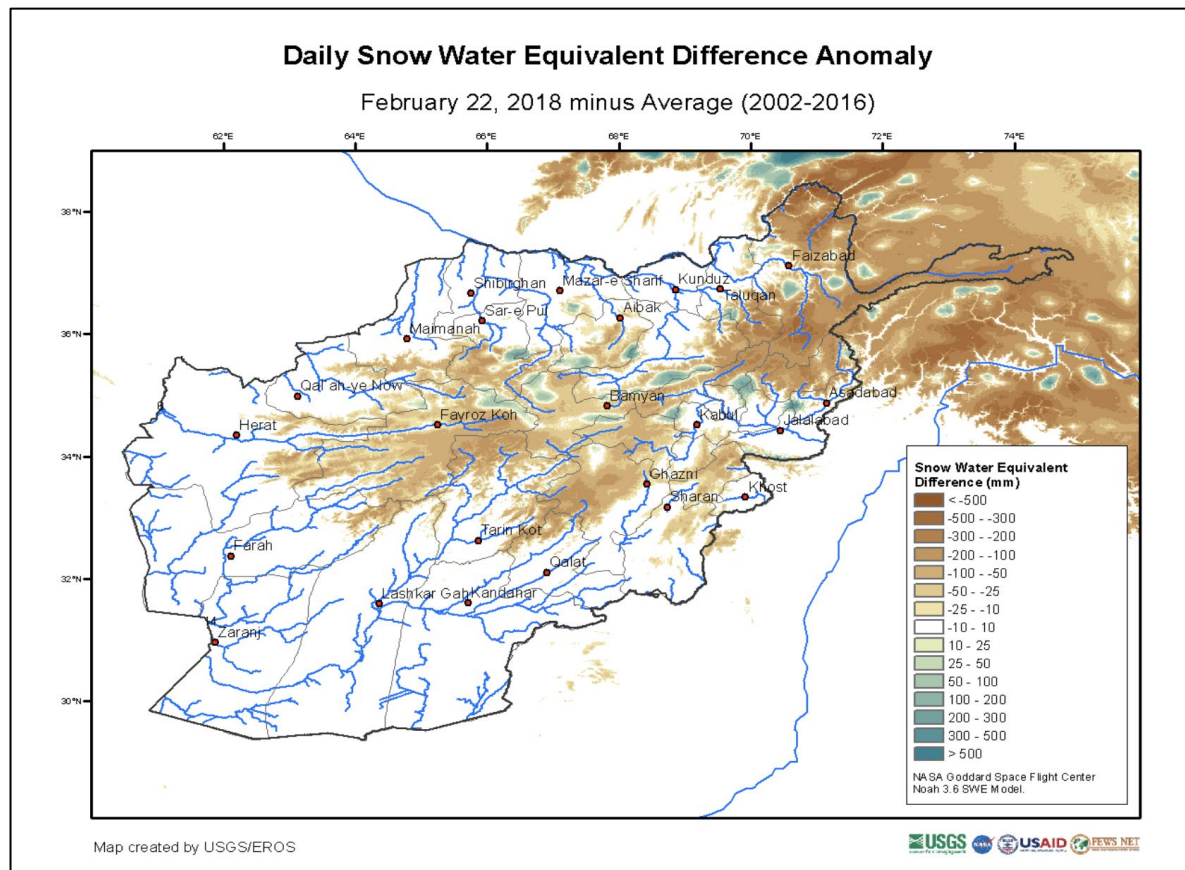
515
516 A La Niña Watch was issued by NOAA in September 2017 (NOAA, 2017). The FEWS NET
517 October 2017 Food Security Outlook (FEWS NET, 2017a) stated that La Niña conditions were
518 expected throughout the northern hemisphere fall and winter and that below-average precipitation
519 was likely over much of Central Asia, including Afghanistan, during the 2017-2018 wet season.
520 With the expectation of below average precipitation coupled with above average temperatures,
521 FEWS NET anticipated that snowpack would most likely be below average. In the context of food
522 security outcomes, it was assumed that areas planted with winter wheat were likely to be less than
523 usual, reducing land preparation activities and associated demand for labor. Two provinces of
524 particular concern were Daykundi and Wardak (Fig. 8a brown borders), both located in the
525 Helmand River Basin (Fig. 8a; gray shading). Precipitation deficits in these provinces would lead to
526 poor rangeland resources and pasture availability and would likely result in decreased livestock
527 productivity and milk production through May. However, given that October was the start of the wet
528 season, there remained a large spread of possible outcomes: spatial and temporal rainfall
529 distributions, and snowpack totals necessitating routine updates to assumptions.

530
531 Monitoring continued during the wet season, tracking observations from remote sensing, models,
532 and field reports as well as forecasts across timescales. This information was used to regularly
533 update expectations of end of season outcomes. Using the FLDAS Central Asia data stream, a
534 December 21, 2017, NOAA CPC Weather Hazards Brief reported that parts of northern and central
535 Afghanistan remained atypically snow free, and north-eastern high elevation areas exhibited SWE
536 deficits. SWE is a commonly used measurement of the amount of liquid water contained within the
537 snowpack, and an indicator of the amount of water that will be released from the snowpack when it
538 melts. By January 17, 2018, an abnormal dryness polygon was placed over northeastern Afghanistan
539 and the central highlands, based on below-average SWE values from the FLDAS Central Asia
540 estimates. Abnormal dryness is defined for an area that has registered cumulative 4-week
541 precipitation and soil moisture ranking less than the 30th percentile, with a Standardized
542 Precipitation Index (SPI) of 0.4 standard deviation below the average. In addition, it is required that
543 forecasts indicate below-average precipitation (less than 80% of normal) for that area during the 1-
544 week outlook period. By late February 2018, precipitation deficits and related SWE (Fig. 9)
545 increased and met the criteria for “drought” (Fig. 8b). Drought is defined as an area that has
546 previously been defined as “Abnormal Dryness” and has continued to register seasonal precipitation
547 and soil moisture deficits since the beginning of the rainfall season. Specifically, an eight-week
548 cumulative precipitation, soil moisture, and runoff below the 20th percentile rank, and an SPI of 0.8
549 standard deviation below the average are classification guidelines.

550



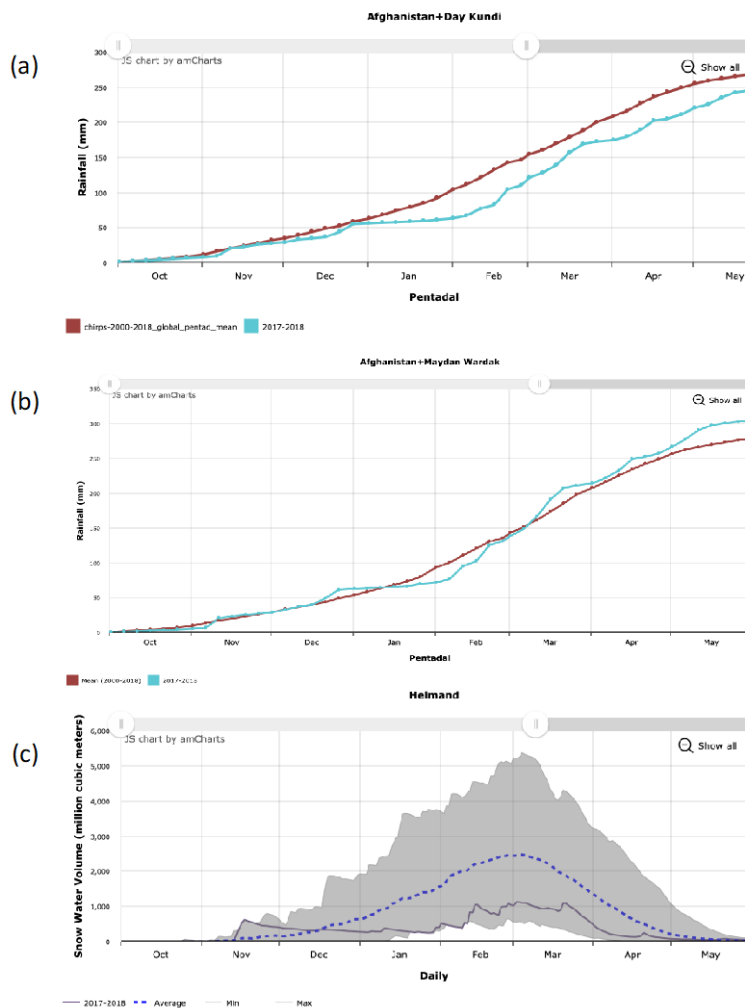
551
552 Figure 8. (a) Map showing hydrological basins, with Helmand Basin in darker gray and location of
553 Daykundi and Wardak provinces (outlined in red) where food security conditions were of particular
554 concern, (b) NOAA CPC Afghanistan Hazards Report for February 22-28, 2018 (CPC NOAA,
555 2018) showing widespread abnormal dryness and drought, defined by 90-day precipitation deficits
556 and extremely low snow water equivalent.
557



558
559 Figure 9. FLDAS Central Asia snow water equivalent (SWE) estimates for February 22, 2018.
560 SWE deficits of 300-mm were widespread at this time.
561

562 The February 2018 Food Security Outlook (FEWS NET, 2018b) provided the following updates,
563 based on the CPC Hazards Reports and Seasonal Monitors: “Snow accumulation and cumulative
564 precipitation were well below average for the season through February 2018, with some basins at or
565 near record low snowpack, with data since 2002....These factors will likely have an adverse impact
566 on staple production in marginal irrigated areas and in many rainfed areas. [Moreover, with]
567 forecasts for above-average temperatures during the spring and summer, rangeland conditions are
568 expected to be poor during the period of analysis through September 2018. This could have an
569 adverse impact on pastoralists and agro-pastoralists, particularly in areas where livestock
570 movements are limited by conflict.” The Crop Monitor for Early Warning reports for February and
571 March 2018 (GEOGLAM, 2018a, b) also cited reduced snowpack in Afghanistan and the negative
572 impacts on winter wheat crops as well as irrigation water availability in the Spring. The story was
573 also highlighted in NASA Earth Observatory March 2018 “Record Low Snowpack in Afghanistan”
574 (NASA Earth Observatory, 2018).
575

576 The USGS Early Warning eXplorer (EWX) (Shukla et al., 2021) allows analysts to look at maps
 577 and time series for a variety of variables and specific provinces and river basins. Plots from EWX in
 578 Fig. 10 show below average precipitation for provinces in the Helmand Basin for January and
 579 February. CHIRPS cumulative rainfall for 2017-18 versus the 18-year average for Day Kundi (a.k.a.
 580 Daykundi) Province showed near average conditions until December. From January, cumulative
 581 rainfall remained below the 2000-2018 average throughout the rest of the season ending in May; the
 582 same pattern occurred in nearby Uruzgan Province. In neighboring Maydan Wardak (a.k.a Wardak)
 583 Province, below average conditions were experienced in January and February, but cumulative
 584 rainfall recovered in March to remain slightly above average. Day Kundi (Fig. 10b) and Wardak
 585 (Fig. 10c) are provinces located in the upper reaches of the Helmand Basin. Fig. 10c shows SWE
 586 averaged across the entire Helmand basin. The gray shading indicates the range of the minimum and
 587 maximum values, and the dashed blue line is the average. Initial snow conditions start above
 588 average until December, after which SWE deficits are near record low values through the beginning
 589 of February, and then persist at below-average levels.



590

591 Figure 10. (a) CHIRPS cumulative rainfall for 2017-18 versus average conditions for Daykundi
592 Province. (b) CHIRPS cumulative rainfall for 2017-18 versus average conditions for Maydan
593 Wardak Province (c) Helmand Basin SWE from the FLDAS Central Asia data stream. The grey
594 shading indicates the range of the minimum and maximum values, dashed blue line is the average,
595 and black line is 2017-18. Figures from USGS EWX (<https://earlywarning.usgs.gov/fews/ewx/>).

596
597 By the end of the season in April 2018, FEWS NET (2018c) concluded that “below-average
598 precipitation throughout most of the country during the October 2017 – May 2018 wet season has
599 led to very low snowpack ...Low irrigation water availability is likely to have an adverse impact on
600 yields for winter wheat and other ...barley, maize, and others.. particularly in downstream areas in
601 regions with limited rainfall. ...The poor performance of the wet season and above average
602 temperatures... exacerbated dry rangeland conditions in many areas, particularly in ...Sari Pul, [and
603 surrounding] ...provinces. Pastoralists and agropastoralists in these areas will likely attempt to
604 migrate to areas with better pasture and water availability or sell livestock at below-average prices.”
605 At the same time, UNICEF (2018) reported in April 2018 that among “the [drought] affected
606 provinces, Baghis, Bamyán, Daykundi, Ghor, Helmand, ... and Uruzgan are of critical priority for
607 nutrition and water, sanitation and hygiene assistance.”

608
609 Several months after a season has ended, and harvest is complete, more statistics become available
610 for further verification of the drought outcomes. The FEWS NET October 2018 Food Security
611 Outlook (2018a) reported that the 2017-18 drought had significant negative impacts on rainfed
612 wheat production and livestock pasture and body conditions across the country. Reporting statistics
613 from the Afghanistan Ministry of Agriculture, Irrigation, and Livestock, the total wheat production
614 for the 2017-18 season was about 20% below average, where irrigated agriculture performed about
615 average. However, rainfed agricultural production was only about 50% of average, most severely
616 affecting households in Badakhshan, Badhis, and Daykundi provinces. In these locations dry
617 conditions, conflict, poor incomes, and depleted assets were expected to continue to face emergency
618 food insecurity through May 2019.

619 **5. Data Availability**

620 The Central Asia data described in this manuscript can be accessed at the NASA GES DISC
621 repository under data doi 10.5067/VQ4CD3Y9YC0R. The data citation is the following:

622
623 Jacob, Jossy and Slinski, Kimberly (NASA/GSFC/HSL) (2021), FLDAS Noah Land Surface Model
624 L4 Central Asia Daily 0.01 x 0.01 degree, Greenbelt, MD, USA, Goddard Earth Sciences Data and
625 Information Services Center (GES DISC) 10.5067/VQ4CD3Y9YC0R

626
627 The global data described in this manuscript can be accessed at the NASA GES DISC repository
628 under data doi 10.5067/5NHC22T9375G. The data citation is the following:

629

630 McNally, Amy. NASA/GSFC/HSL (2018), FLDAS Noah Land Surface Model L4 Global Monthly
631 0.1 x 0.1 degree (MERRA-2 and CHIRPS), Greenbelt, MD, USA, Goddard Earth Sciences Data and
632 Information Services Center (GES DISC), 10.5067/5NHC22T9375G

633
634 Currently the USGS EROS Center provides images from these data:
635 <https://earlywarning.usgs.gov/fews/search/Asia/Central%20Asia>, as well as an interactive data
636 viewer, the USGS EWX (<https://earlywarning.usgs.gov/fews/ewx/>).

637 **6. Code availability**

638 The NASA Land Information System Framework (LISF) is publicly available and an open-source
639 software. The software and technical support are available at <https://github.com/NASA-LIS/LISF>.
640 The version used for this paper was LISF-public-7.3.2 <https://doi.org/10.5281/zenodo.6795120>.

641 **7. Conclusion**

642 This paper describes a comprehensive hydrologic analysis system for food security monitoring in
643 Central Asia, with analysis focusing on Afghanistan. While these data are tailored to specific needs,
644 they are also applicable to other climate services and research. Our intent is to provide the reader
645 with information regarding the configuration and specification of both the current global and Central
646 Asia data streams. These data are publicly available and available at near-real time for food security
647 decision support. Note that, as an on-going initiative, FLDAS model version and parameters are
648 routinely updated, and the user should consult the version updates provided by the NASA Goddard
649 Earth Science Data and Information Services Center (GES DISC) data provider and documentation
650 on USGS Early Warning website. For example, efforts are currently underway to upgrade to the
651 Noah-MP (Niu et al., 2011) land surface model, which requires some changes in parameters for
652 snow, glaciers and groundwater. This, and future changes, can be informed by the strengths and
653 weaknesses of the data stream configurations that we have discussed in this paper.

654
655 This paper also provides model-model and model-remote sensing comparisons as well as a review
656 of other research that highlights the challenges of quantitative evaluation of models and remote
657 sensing in this region. A key challenge to hydrologic modeling is the considerable uncertainty in the
658 meteorological forcing available for this region, particularly precipitation. Advancements in remote
659 sensing and modeling should help reduce these uncertainties. In addition, the current land surface
660 modeling reflects natural conditions, i.e., they do not include representation of anthropogenic effects
661 such as human water abstractions (e.g., dams for flood control or irrigation, water diversions,
662 groundwater pumping) or land application of abstracted water (i.e., irrigation). These factors affect
663 estimates of runoff, soil moisture, evapotranspiration, and sensible heat flux (land surface
664 temperatures) in irrigated areas. Therefore, it is important to be aware of the limitations and
665 combine with other products (e.g., NDVI or Actual Evapotranspiration (ETa) in irrigated areas)
666 when exploring water and energy balance. Even with improvements to meteorological forcing and

667 modeling parameterizations, errors will remain. Therefore, the ‘convergence of evidence’ approach
668 is beneficial and would be important when assessing hydro-meteorological hazards and associated
669 risks to food and water security. By making the data publicly available the broader food security and
670 water resources communities will be able to provide insights that can lead to improvements in our
671 understanding of the water and energy balance that can ultimately lead to improvements to food and
672 water security decision support systems.

673

674 **8. Author contribution**

675 JJ runs the code, updates websites, and archives routinely. DS maintains LISF code used in paper,
676 JJ, KA, DS, SP conducted model evaluation AM, KS, CPL, SK contributed to design of evaluation.
677 JR, MB, SP manage the data for USGS distribution. AH, JV provide feedback on data quality and
678 interpretation. AM prepared the manuscript with contributions from all co-authors.

679 **9. Acknowledgements**

680 The authors wish to acknowledge the original version of the Central Asia snow modeling with LIS6
681 performed at NOAA National Operational Hydrologic Remote Sensing Center by Greg Fall and
682 Logan Karsten. USGS work was performed under U.S. Agency for International Development
683 (USAID), Bureau of Humanitarian Assistance (BHA) PAPA AID-FFP-T-17-00003 and USGS
684 contract 140G0119C0001. Any use of trade, firm, or product names is for descriptive purposes only
685 and does not imply endorsement by the U.S. Government. KS, AH, DS, JJ, NASA work was
686 performed under USAID BHA PAPA AID-FFP-T-17-00001. KS, AH acknowledge support from
687 the NASA Harvest Consortium (NASA Applied Sciences Grant No. 80NSSC17K0625). Computing
688 resources have been provided by NASA’s Center for Climate Simulation (NCCS). Distribution of
689 data from the Goddard Earth Sciences Data and Information Services Center (GES DISC) is funded
690 by NASA's Science Mission Directorate (SMD). We thank NOAA CPC International Desk for use
691 of figures, and the NASA Land Information System Team for software support and development.
692 The authors also thank the USGS reviewer for comments that improved the quality of the
693 manuscript.

694 **10. References**

695 Arsenault, K. R., Houser, P. R., and De Lannoy, G. J. M.: Evaluation of the MODIS snow cover
696 fraction product: Satellite-based snow cover fraction evaluation., *Hydrol. Process.*, 28, 980–998,
697 <https://doi.org/10.1002/hyp.9636>, 2014.

698 Arsenault, K. R., Kumar, S. V., Geiger, J. V., Wang, S., Kemp, E., Mocko, D. M., Beaudoin, H.
699 K., Getirana, A., Navari, M., Li, B., Jacob, J., Wegiel, J., and Peters-Lidard, C. D.: The Land
700 Surface Data Toolkit (LDT v7.2) - A Data Fusion Environment for Land Data Assimilation
701 Systems, *Geosci. Model Dev.*, 11, <https://doi.org/10.5194/gmd-11-3605-2018>, 2018.

- 702 Barlage, M., Zeng, X., Wei, H., and Mitchell, K. E.: A global 0.05° maximum albedo dataset of
703 snow-covered land based on MODIS observations: Maximum Albedo of Snow-covered, *Geophys.*
704 *Res. Lett.*, 32, <https://doi.org/10.1029/2005GL022881>, 2005.
- 705 Barlow, M., Wheeler, M., Lyon, B., and Cullen, H.: Modulation of Daily Precipitation over
706 Southwest Asia by the Madden–Julian Oscillation, *Monthly Weather Review*, 133, 3579–3594,
707 <https://doi.org/10.1175/MWR3026.1>, 2005.
- 708 Barlow, M., Zaitchik, B., Paz, S., Black, E., Evans, J., and Hoell, A.: A Review of Drought in the
709 Middle East and Southwest Asia, *Journal of Climate*, 29, 8547–8574, <https://doi.org/10.1175/JCLI->
710 [D-13-00692.1](https://doi.org/10.1175/JCLI-D-13-00692.1), 2016.
- 711 Carroll, M., DiMiceli, C., Wooten, M., Hubbard, A., Sohlberg, R., and Townshend, J.: MOD44W
712 MODIS/Terra Land Water Mask Derived from MODIS and SRTM L3 Global 250m SIN Grid V006
713 [Data set]. NASA EOSDIS Land Processes DAAC., 2017.
- 714 Chen, F., Mitchell, K., Schaake, J., Xue, Y., Pan, H.-L., Koren, V., Duan, Q. Y., Ek, M., and Betts,
715 A.: Modeling of land surface evaporation by four schemes and comparison with FIFE observations,
716 *J. Geophys. Res.*, 101, 7251–7268, <https://doi.org/10.1029/95JD02165>, 1996.
- 717 CIA World Factbook: <https://www.cia.gov/the-world-factbook/countries/afghanistan/#introduction>.
- 718 Cosgrove, B. A., Lohmann, D., Mitchell, K. E., Houser, P. R., Wood, E. F., Schaake, J. C., Robock,
719 A., Marshall, C., Sheffield, J., Duan, Q., Luo, L., Higgins, R. W., Pinker, R. T., Tarpley, J. D., and
720 Meng, J.: Real-time and retrospective forcing in the North American Land Data Assimilation
721 System (NLDAS) project, *J. Geophys. Res.*, 108, 2002JD003118,
722 <https://doi.org/10.1029/2002JD003118>, 2003.
- 723 CPC NOAA: Weather Hazards Outlook of Afghanistan and Central Asia for the Period of February
724 22 - 28, 2018, 2018.
- 725 Csiszar, I. and Gutman, G.: Mapping global land surface albedo from NOAA AVHRR, 104, 6215–
726 6228, <https://doi.org/10.1029/1998JD200090>, 1999.
- 727 Davenport, F. M., Harrison, L., Shukla, S., Husak, G., Funk, C., and McNally, A.: Using out-of-
728 sample yield forecast experiments to evaluate which earth observation products best indicate end of
729 season maize yields, *Environ. Res. Lett.*, 14, 124095, <https://doi.org/10.1088/1748-9326/ab5ccd>,
730 2019.
- 731 Derber, J. C., Parrish, D. F., and Lord, S. J.: The New Global Operational Analysis System at the
732 National Meteorological Center, *Weather and Forecasting*, 6, 538–547,
733 [https://doi.org/10.1175/1520-0434\(1991\)006<0538:TNGOAS>2.0.CO;2](https://doi.org/10.1175/1520-0434(1991)006<0538:TNGOAS>2.0.CO;2), 1991.

- 734 Dezfuli, A. K., Ichoku, C. M., Huffman, G. J., Mohr, K. I., Selker, J. S., van de Giesen, N.,
735 Hochreutener, R., and Annor, F. O.: Validation of IMERG Precipitation in Africa, *Journal of*
736 *Hydrometeorology*, 18, 2817–2825, <https://doi.org/10.1175/JHM-D-17-0139.1>, 2017.
- 737 Ek, M. B., Mitchell, K. E., Lin, Y., Rogers, E., Grunmann, P., Koren, V., Gayno, G., and Tarpley, J.
738 D.: Implementation of Noah land surface model advances in the National Centers for Environmental
739 Prediction operational mesoscale Eta model, *JGR: Atmospheres*, 108,
740 <https://doi.org/10.1029/2002JD003296>, 2003.
- 741 Ellenburg, W. L., Mishra, V., Roberts, J. B., Limaye, A. S., Case, J. L., Blankenship, C. B., and
742 Cressman, K.: Detecting Desert Locust Breeding Grounds: A Satellite-Assisted Modeling
743 Approach, *Remote Sensing*, 13, 1276, <https://doi.org/10.3390/rs13071276>, 2021.
- 744 Entekhabi, D., Njoku, E. G., O’Neill, P. E., Kellogg, K. H., Crow, W. T., Edelstein, W. N., Entin, J.
745 K., Goodman, S. D., Jackson, T. J., Johnson, J., Kimball, J., Piepmeier, J. R., Koster, R. D., Martin,
746 N., McDonald, K. C., Moghaddam, M., Moran, S., Reichle, R., Shi, J. C., Spencer, M. W.,
747 Thurman, S. W., Tsang, L., and Zyl, J. V.: The Soil Moisture Active Passive (SMAP) Mission, 98,
748 704–716, <https://doi.org/10.1109/JPROC.2010.2043918>, 2010.
- 749 Entekhabi, D., Das, N., Njoku, E. G., Johnson, J., and Shi, J. C.: SMAP L3 Radar/Radiometer
750 Global Daily 9 km EASE-Grid Soil Moisture, Version 3, NASA National Snow and Ice Data Center
751 DAAC [preprint], <https://doi.org/10.5067/7KKNQ5UURM2W>, 2016.
- 752 FEWS NET: Afghanistan Food Security Outlook October 2017-May 2018 Conflict, dry spells, and
753 weak labor opportunities will lead to deterioration in outcomes during 2018 lean season, 2017a.
- 754 FEWS NET: Update on performance of the October 2016 – May 2017 wet season, 2017b.
- 755 FEWS NET: Afghanistan Food Security Outlook: Emergency assistance needs are atypically high
756 through the lean season across the country, FEWS NET, 2018a.
- 757 FEWS NET: Afghanistan Food Security Outlook February to September 2018: Low snow
758 accumulation and dry soil conditions likely to impact 2018 staple production, 2018b.
- 759 FEWS NET: Afghanistan Food Security Outlook Update April 2018: Poor rangeland conditions and
760 below-average water availability will limit seasonal improvements, 2018c.
- 761 FEWS NET: El Niño and Precipitation, FEWS NET, <https://fews.net/el-ni%C3%B1o-and-precipitation>, 2020a.
- 762
- 763 FEWS NET: La Niña and Precipitation, FEWS NET, <https://fews.net/la-ni%C3%B1a-and-precipitation>, 2020b.
- 764

- 765 FEWS NET: Afghanistan Food Security Outlook February to September 2021: Below-average
766 precipitation likely to drive below-average agricultural and livestock production in 2021, 2021.
- 767 Funk, C., Peterson, P., Landsfeld, M., Pedreros, D., Verdin, J., Shukla, S., Husak, G., Rowland, J.,
768 Harrison, L., Hoell, A., and Michaelsen, J.: The climate hazards infrared precipitation with stations--
769 a new environmental record for monitoring extremes., The climate hazards infrared precipitation
770 with stations—a new environmental record for monitoring extremes, *Sci Data*, 2, 2, 150066–
771 150066, <https://doi.org/10.1038/sdata.2015.66>, 10.1038/sdata.2015.66, 2015.
- 772 Funk, C. C., Peterson, P., Huffman, G. J., Landsfeld, M. F., Peters-Lidard, C., Davenport, F.,
773 Shukla, S., Peterson, S., Pedreros, D. H., Ruane, A. C., Mutter, C., Turner, W., Harrison, L.,
774 Sonnier, A., Way-Henthorne, J., and Husak, G. J.: Introducing and Evaluating the Climate Hazards
775 Center IMERG with Stations (CHIMES): Timely Station-Enhanced Integrated Multisatellite
776 Retrievals for Global Precipitation Measurement, 103, E429–E454, [https://doi.org/10.1175/BAMS-](https://doi.org/10.1175/BAMS-D-20-0245.1)
777 [D-20-0245.1](https://doi.org/10.1175/BAMS-D-20-0245.1), 2022.
- 778 Gadelha, A. N., Coelho, V. H. R., Xavier, A. C., Barbosa, L. R., Melo, D. C. D., Xuan, Y.,
779 Huffman, G. J., Petersen, W. A., and Almeida, C. das N.: Grid box-level evaluation of IMERG over
780 Brazil at various space and time scales, *Atmospheric Research*, 218, 231–244,
781 <https://doi.org/10.1016/j.atmosres.2018.12.001>, 2019.
- 782 Gelaro, R., McCarty, W., Suárez, M. J., Todling, R., Molod, A., Takacs, L., Randles, C. A.,
783 Darmenov, A., Bosilovich, M. G., Reichle, R., Wargan, K., Coy, L., Cullather, R., Draper, C.,
784 Akella, S., Buchard, V., Conaty, A., da Silva, A. M., Gu, W., Kim, G.-K., Koster, R., Lucchesi, R.,
785 Merkova, D., Nielsen, J. E., Partyka, G., Pawson, S., Putman, W., Rienecker, M., Schubert, S. D.,
786 Sienkiewicz, M., and Zhao, B.: The Modern-Era Retrospective Analysis for Research and
787 Applications, Version 2 (MERRA-2), *J. Climate*, 30, 5419–5454, [https://doi.org/10.1175/JCLI-D-](https://doi.org/10.1175/JCLI-D-16-0758.1)
788 [16-0758.1](https://doi.org/10.1175/JCLI-D-16-0758.1), 2017.
- 789 GEOGLAM: Early Warning Crop Monitor February 2018,
790 https://cropmonitor.org/documents/EWCM/reports/EarlyWarning_CropMonitor_201802.pdf,
791 2018a.
- 792 GEOGLAM: Early Warning Crop Monitor March 2018,
793 https://cropmonitor.org/documents/EWCM/reports/EarlyWarning_CropMonitor_201802.pdf,
794 2018b.
- 795 Ghatak, D., Zaitchik, B., Kumar, S., Matin, M. A., Bajracharya, B., Hain, C., and Anderson, M.:
796 Influence of Precipitation Forcing Uncertainty on Hydrological Simulations with the NASA South
797 Asia Land Data Assimilation System, *Hydrology*, 5, 57, <https://doi.org/10.3390/hydrology5040057>,
798 2018.

- 799 Grace, K. and Davenport, F.: Climate variability and health in extremely vulnerable communities:
800 investigating variations in surface water conditions and food security in the West African Sahel,
801 *Population & Environment*, 42, 553–577, <https://doi.org/10.1007/s11111-021-00375-9>, 2021.
- 802 Gutman, G. and Ignatov, A.: The derivation of the green vegetation fraction from NOAA/AVHRR
803 data for use in numerical weather prediction models, *International Journal of Remote Sensing*, 19,
804 1533–1543, <https://doi.org/10.1080/014311698215333>, 1998.
- 805 Hall, D. and Riggs, G.: MODIS/Terra Snow Cover Daily L3 Global 500m SIN Grid version 6,
806 <https://doi.org/10.5067/MODIS/MOD10A1.006>, 2016.
- 807 Hengl, T., Jesus, J. M. de, Heuvelink, G. B. M., Gonzalez, M. R., Kilibarda, M., Blagotić, A.,
808 Shangguan, W., Wright, M. N., Geng, X., Bauer-Marschallinger, B., Guevara, M. A., Vargas, R.,
809 MacMillan, R. A., Batjes, N. H., Leenaars, J. G. B., Ribeiro, E., Wheeler, I., Mantel, S., and
810 Kempen, B.: SoilGrids250m: Global gridded soil information based on machine learning, *PLOS*
811 *ONE*, 12, e0169748, <https://doi.org/10.1371/journal.pone.0169748>, 2017.
- 812 Hewitt, C., Mason, S., and Walland, D.: The Global Framework for Climate Services, *Nature Clim*
813 *Change*, 2, 831–832, <https://doi.org/10.1038/nclimate1745>, 2012.
- 814 Hoell, A., Funk, C., and Barlow, M.: The Forcing of Southwestern Asia Teleconnections by Low-
815 Frequency Sea Surface Temperature Variability during Boreal Winter, *J. Climate*, 28, 1511–1526,
816 <https://doi.org/10.1175/JCLI-D-14-00344.1>, 2015.
- 817 Hoell, A., Barlow, M., Cannon, F., and Xu, T.: Oceanic Origins of Historical Southwest Asia
818 Precipitation During the Boreal Cold Season, *J. Climate*, 30, 2885–2903,
819 <https://doi.org/10.1175/JCLI-D-16-0519.1>, 2017.
- 820 Hoell, A., Cannon, F., and Barlow, M.: Middle East and Southwest Asia Daily Precipitation
821 Characteristics Associated with the Madden–Julian Oscillation during Boreal Winter, *J. Climate*, 31,
822 8843–8860, <https://doi.org/10.1175/JCLI-D-18-0059.1>, 2018.
- 823 Hoell, A., Eischeid, J., Barlow, M., and McNally, A.: Characteristics, precursors, and potential
824 predictability of Amu Darya Drought in an Earth system model large ensemble, *Clim Dyn*, 55,
825 2185–2206, <https://doi.org/10.1007/s00382-020-05381-5>, 2020.
- 826 Huffman, G. J., Bolvin, D. T., Braithwaite, D., Hsu, K.-L., Joyce, R. J., Kidd, C., Nelkin, E. J.,
827 Sorooshian, S., Stocker, E. F., Tan, J., Wolff, D. B., and Xie, P.: Integrated Multi-satellite Retrievals
828 for the Global Precipitation Measurement (GPM) Mission (IMERG), in: *Satellite Precipitation*
829 *Measurement: Volume 1*, edited by: Levizzani, V., Kidd, C., Kirschbaum, D. B., Kummerow, C. D.,
830 Nakamura, K., and Turk, F. J., Springer International Publishing, Cham, 343–353,
831 https://doi.org/10.1007/978-3-030-24568-9_19, 2020.

- 832 Immerzeel, W. W., Wanders, N., Lutz, A. F., Shea, J. M., and Bierkens, M. F. P.: Reconciling high-
833 altitude precipitation in the upper Indus basin with glacier mass balances and runoff, *Hydrol. Earth*
834 *Syst. Sci.*, 19, 4673–4687, <https://doi.org/10.5194/hess-19-4673-2015>, 2015.
- 835 Jacob, J. and Slinski, K.: GES DISC Dataset: FLDAS Noah Land Surface Model L4 Central Asia
836 Daily 0.01 x 0.01 degree (FLDAS_NOAH001_G_CA_D 001),
837 <https://doi.org/10.5067/VQ4CD3Y9YC0R>, 2021.
- 838 Jung, H. C., Getirana, A., Policelli, F., McNally, A., Arsenault, K. R., Kumar, S., Tadesse, T., and
839 Peters-Lidard, C. D.: Upper Blue Nile basin water budget from a multi-model perspective, *Journal*
840 *of Hydrology*, 555, 535–546, <https://doi.org/10.1016/j.jhydrol.2017.10.040>, 2017.
- 841 Jung, H. C., Getirana, A., Arsenault, K. R., Holmes, T. R. H., and McNally, A.: Uncertainties in
842 Evapotranspiration Estimates over West Africa, *Remote Sensing*, 11, 892,
843 <https://doi.org/10.3390/rs11080892>, 2019.
- 844 Kato, H. and Rodell, M.: Sensitivity of Land Surface Simulations to Model Physics, Land
845 Characteristics, and Forcings, at Four CEOP Sites, *Journal of the Meteorological Society of Japan.*
846 *Ser. II, Volume 85A*, 187–204, <https://doi.org/10.2151/jmsj.85A.187>, 2007.
- 847 Kirschbaum, D. B., Huffman, G. J., Adler, R. F., Braun, S., Garrett, K., Jones, E., McNally, A.,
848 Skofronick-Jackson, G., Stocker, E., Wu, H., and Zaitchik, B. F.: NASA’s Remotely Sensed
849 Precipitation: A Reservoir for Applications Users, *Bull. Amer. Meteor. Soc.*, 98, 1169–1184,
850 <https://doi.org/10.1175/BAMS-D-15-00296.1>, 2016.
- 851 Kumar, S. V., Peters-Lidard, C. D., Tian, Y., Houser, P. R., Geiger, J., Olden, S., Lighty, L.,
852 Eastman, J. L., Doty, B., Dirmeyer, P., Adams, J., Mitchell, K., Wood, E. F., and Sheffield, J.: Land
853 information system: An interoperable framework for high resolution land surface modeling,
854 *Environmental Modelling & Software*, 21, 1402–1415,
855 <https://doi.org/10.1016/j.envsoft.2005.07.004>, 2006.
- 856 Kumar, S. V., Peters-Lidard, C. D., Santanello, J., Harrison, K., Liu, Y., and Shaw, M.: Land
857 surface Verification Toolkit (LVT) – a generalized framework for land surface model evaluation,
858 *Geosci. Model Dev.*, 5, 869–886, <https://doi.org/10.5194/gmd-5-869-2012>, 2012.
- 859 Kumar, S. V., Peters-Lidard, C. D., Mocko, D., and Tian, Y.: Multiscale Evaluation of the
860 Improvements in Surface Snow Simulation through Terrain Adjustments to Radiation, *Journal of*
861 *Hydrometeorology*, 14, 220–232, <https://doi.org/10.1175/JHM-D-12-046.1>, 2013.
- 862 Ma, Z., Xu, J., Zhu, S., Yang, J., Tang, G., Yang, Y., Shi, Z., and Hong, Y.: AIMERG: a new Asian
863 precipitation dataset (0.1°/half-hourly, 2000–2015) by calibrating the GPM-era IMERG at a daily
864 scale using APHRODITE, *Earth Syst. Sci. Data*, 12, 1525–1544, [https://doi.org/10.5194/essd-12-](https://doi.org/10.5194/essd-12-1525-2020)
865 [1525-2020](https://doi.org/10.5194/essd-12-1525-2020), 2020.

- 866 Manz, B., Páez-Bimos, S., Horna, N., Buytaert, W., Ochoa-Tocachi, B., Lavado-Casimiro, W., and
867 Willems, B.: Comparative Ground Validation of IMERG and TMPA at Variable Spatiotemporal
868 Scales in the Tropical Andes, *Journal of Hydrometeorology*, 18, 2469–2489,
869 <https://doi.org/10.1175/JHM-D-16-0277.1>, 2017.
- 870 McNally, A.: GES DISC Dataset: FLDAS Noah Land Surface Model L4 Global Monthly 0.1 x 0.1
871 degree (MERRA-2 and CHIRPS) (FLDAS_NOAH01_C_GL_M 001), 2018.
- 872 McNally, A., Husak, G. J., Brown, M., Carroll, M., Funk, C., Yatheendradas, S., Arsenault, K.,
873 Peters-Lidard, C., and Verdin, J. P.: Calculating Crop Water Requirement Satisfaction in the West
874 Africa Sahel with Remotely Sensed Soil Moisture, *J. Hydrometeor.*, 16, 295–305,
875 <https://doi.org/10.1175/JHM-D-14-0049.1>, 2015.
- 876 McNally, A., Shukla, S., Arsenault, K. R., Wang, S., Peters-Lidard, C. D., and Verdin, J. P.:
877 Evaluating ESA CCI soil moisture in East Africa, *International Journal of Applied Earth
878 Observation and Geoinformation*, 48, 96–109, <https://doi.org/10.1016/j.jag.2016.01.001>, 2016.
- 879 McNally, A., Arsenault, K., Kumar, S., Shukla, S., Peterson, P., Wang, S., Funk, C., Peters-lidard,
880 C. D., and Verdin, J. P.: A land data assimilation system for sub-Saharan Africa food and water
881 security applications, *Scientific Data*, 4, 170012, <http://dx.doi.org/10.1038/sdata.2017.12>, 2017.
- 882 McNally, A., McCartney, S., Ruane, A. C., Mladenova, I. E., Whitcraft, A. K., Becker-Reshef, I.,
883 Bolten, J. D., Peters-Lidard, C. D., Rosenzweig, C., and Uz, S. S.: Hydrologic and Agricultural
884 Earth Observations and Modeling for the Water-Food Nexus, *Front. Environ. Sci.*, 7,
885 <https://doi.org/10.3389/fenvs.2019.00023>, 2019.
- 886 Miller, J., Barlage, M., Zeng, X., Wei, H., Mitchell, K., and Tarpley, D.: Sensitivity of the
887 NCEP/Noah land surface model to the MODIS green vegetation fraction data set, *Geophys. Res.
888 Lett.*, 33, <https://doi.org/10.1029/2006GL026636>, 2006.
- 889 Molteni, F., Buizza, R., Palmer, T. N., and Petroliagis, T.: The ECMWF Ensemble Prediction
890 System: Methodology and validation, *Q J R Meteorol Soc*, 122, 73–119,
891 <https://doi.org/10.1002/qj.49712252905>, 1996.
- 892 NASA Earth Observatory: Record Low Snowpack in Afghanistan, NASA Earth Observatory, 2018.
- 893 NASA JPL: NASA Shuttle Radar Topography Mission Global 30 arc second [Data set]. NASA
894 EOSDIS Land Processes DAAC, NASA EOSDIS Land Processes DAAC, NASA EOSDIS Land
895 Processes DAAC., 2013.
- 896 Nazemosadat, M. J. and Ghaedamini, H.: On the Relationships between the Madden–Julian
897 Oscillation and Precipitation Variability in Southern Iran and the Arabian Peninsula: Atmospheric
898 Circulation Analysis, 23, 887–904, <https://doi.org/10.1175/2009JCLI2141.1>, 2010.

- 899 NCAR Research Applications Library: <https://ral.ucar.edu/solutions/products/unified-noah-lsm>, last
900 access: 12 November 2021.
- 901 Niu, G.-Y., Yang, Z.-L., Mitchell, K. E., Chen, F., Ek, M. B., Barlage, M., Kumar, A., Manning, K.,
902 Niyogi, D., Rosero, E., Tewari, M., and Xia, Y.: The community Noah land surface model with
903 multiparameterization options (Noah-MP): 1. Model description and evaluation with local-scale
904 measurements, *JGR: Atmospheres*, 116, <https://doi.org/10.1029/2010JD015139>, 2011.
- 905 NOAA: [https://www.climate.gov/news-features/blogs/enso/september-enso-update-la-ni%C3%B1a-](https://www.climate.gov/news-features/blogs/enso/september-enso-update-la-ni%C3%B1a-watch)
906 [watch](https://www.climate.gov/news-features/blogs/enso/september-enso-update-la-ni%C3%B1a-watch), last access: 12 September 2017.
- 907 NOAA CPC ENSO Cold & Warm Episodes by Season:
908 https://origin.cpc.ncep.noaa.gov/products/analysis_monitoring/ensostuff/ONI_v5.php, last access:
909 29 July 2021.
- 910 Oki, T. and Kanae, S.: Global Hydrological Cycles and World Water Resources, *Science*, 313,
911 1068–1072, <https://doi.org/10.1126/science.1128845>, 2006.
- 912 Pervez, S., McNally, A., Arsenault, K., Budde, M., and Rowland, J.: Vegetation Monitoring
913 Optimization With Normalized Difference Vegetation Index and Evapotranspiration Using Remote
914 Sensing Measurements and Land Surface Models Over East Africa, *Frontiers in Climate*, 3, 1,
915 <https://doi.org/10.3389/fclim.2021.589981>, 2021.
- 916 Peters-Lidard, C. D., Houser, P. R., Tian, Y., Kumar, S. V., Geiger, J., Olden, S., Lighty, L., Doty,
917 B., Dirmeyer, P., Adams, J., Mitchell, K., Wood, E. F., and Sheffield, J.: High-performance Earth
918 system modeling with NASA/GSFC’s Land Information System, *Innovations Syst Softw Eng*, 3,
919 157–165, <https://doi.org/10.1007/s11334-007-0028-x>, 2007.
- 920 Qamer, F. M., Tadesse, T., Matin, M., Ellenburg, W. L., and Zaitchik, B.: Earth Observation and
921 Climate Services for Food Security and Agricultural Decision Making in South and Southeast Asia,
922 *Bull Am Meteorol Soc*, 100, ES171–ES174, <https://doi.org/10.1175/BAMS-D-18-0342.1>, 2019.
- 923 Rana, S., Renwick, J., McGregor, J., and Singh, A.: Seasonal Prediction of Winter Precipitation
924 Anomalies over Central Southwest Asia: A Canonical Correlation Analysis Approach, *J. Climate*,
925 31, 727–741, <https://doi.org/10.1175/JCLI-D-17-0131.1>, 2018.
- 926 Reynolds, C. A., Jackson, T. J., and Rawls, W. J.: Estimating soil water-holding capacities by
927 linking the Food and Agriculture Organization Soil map of the world with global pedon databases
928 and continuous pedotransfer functions, *Water Resources Research*, 36, 3653–3662,
929 <https://doi.org/10.1029/2000WR900130>, 2000.

- 930 Sarmiento, D. P., Slinski, K., McNally, A., Funk, C., Peterson, P., and Peters-Lidard, C. D.: Daily
931 precipitation frequency distributions impacts on land-surface simulations of CONUS, *Front. Water*,
932 0, <https://doi.org/10.3389/frwa.2021.640736>, 2021.
- 933 Schiemann, R., Lüthi, D., Vidale, P. L., and Schär, C.: The precipitation climate of Central Asia—
934 intercomparison of observational and numerical data sources in a remote semiarid region, *Royal*
935 *Meteorological Society*, 28, 295–314, <https://doi.org/10.1002/joc.1532>, 2008.
- 936 Schneider, U., Finger, P., Meyer-Christoffer, A., Rustemeier, E., Ziese, M., and Becker, A.:
937 Evaluating the Hydrological Cycle over Land Using the Newly-Corrected Precipitation Climatology
938 from the Global Precipitation Climatology Centre (GPCC), 8, 52,
939 <https://doi.org/10.3390/atmos8030052>, 2017.
- 940 Senay, G. B., Bohms, S., Singh, R. K., Gowda, P. H., Velpuri, N. M., Alemu, H., and Verdin, J. P.:
941 Operational Evapotranspiration Mapping Using Remote Sensing and Weather Datasets: A New
942 Parameterization for the SSEB Approach, *J Am Water Resour Assoc*, 49, 577–591,
943 <https://doi.org/10.1111/jawr.12057>, 2013.
- 944 Shukla, S., Arsenault, K. R., Hazra, A., Peters-Lidard, C., Koster, R. D., Davenport, F., Magadzire,
945 T., Funk, C., Kumar, S., McNally, A., Getirana, A., Husak, G., Zaitchik, B., Verdin, J., Nsadisa, F.
946 D., and Becker-Reshef, I.: Improving early warning of drought-driven food insecurity in southern
947 Africa using operational hydrological monitoring and forecasting products, *Nat. Hazards Earth Syst.*
948 *Sci.*, 20, 1187–1201, <https://doi.org/10.5194/nhess-20-1187-2020>, 2020.
- 949 Shukla, S., Landsfeld, M., Anthony, M., Budde, M., Husak, G. J., Rowland, J., and Funk, C.:
950 Enhancing the Application of Earth Observations for Improved Environmental Decision-Making
951 Using the Early Warning eXplorer (EWX), *Frontiers in Climate*, 2, 34,
952 <https://doi.org/10.3389/fclim.2020.583509>, 2021.
- 953 Tabar, M., Gluck, J., Goyal, A., Jiang, F., Morr, D., Kehs, A., Lee, D., Hughes, D. P., and Yadav,
954 A.: A PLAN for Tackling the Locust Crisis in East Africa: Harnessing Spatiotemporal Deep Models
955 for Locust Movement Forecasting, in: *Proceedings of the 27th ACM SIGKDD Conference on*
956 *Knowledge Discovery & Data Mining*, New York, NY, USA, 3595–3604,
957 <https://doi.org/10.1145/3447548.3467184>, 2021.
- 958 Tan, J., Petersen, W. A., and Tokay, A.: A Novel Approach to Identify Sources of Errors in IMERG
959 for GPM Ground Validation, *Journal of Hydrometeorology*, 17, 2477–2491,
960 <https://doi.org/10.1175/JHM-D-16-0079.1>, 2016.
- 961 UNICEF: 500,000 children affected by drought in Afghanistan – UNICEF,
962 <https://www.unicef.org/press-releases/500000-children-affected-drought-afghanistan-unicef>, 2018.

- 963 USGS Knowledge Base:
964 <https://earlywarning.usgs.gov/fews/searchkb/Asia/Central%20Asia/Afghanistan>, last access: 12
965 November 2021.
- 966 Vincent, K., Daly, M., Scannell, C., and Leathes, B.: What can climate services learn from theory
967 and practice of co-production?, *Climate Services*, 12, 48–58,
968 <https://doi.org/10.1016/j.cliser.2018.11.001>, 2018.
- 969 Xie, P. and Arkin, P. A.: Analyses of Global Monthly Precipitation Using Gauge Observations,
970 Satellite Estimates, and Numerical Model Predictions, *Journal of Climate*, 9, 840–858,
971 [https://doi.org/10.1175/1520-0442\(1996\)009<0840:AOGMPU>2.0.CO;2](https://doi.org/10.1175/1520-0442(1996)009<0840:AOGMPU>2.0.CO;2), 1996.
- 972 Yatagai, A., Kamiguchi, K., Arakawa, O., Hamada, A., Yasutomi, N., and Kitoh, A.: APHRODITE:
973 Constructing a Long-Term Daily Gridded Precipitation Dataset for Asia Based on a Dense Network
974 of Rain Gauges, *Bull Am Meteorol Soc*, 93, 1401–1415, [https://doi.org/10.1175/BAMS-D-11-](https://doi.org/10.1175/BAMS-D-11-00122.1)
975 [00122.1](https://doi.org/10.1175/BAMS-D-11-00122.1), 2012.
- 976 Yoon, Y., Kumar, S. V., Forman, B. A., Zaitchik, B. F., Kwon, Y., Qian, Y., Rupper, S., Maggioni,
977 V., Houser, P., Kirschbaum, D., Richey, A., Arendt, A., Mocko, D., Jacob, J., Bhanja, S., and
978 Mukherjee, A.: Evaluating the Uncertainty of Terrestrial Water Budget Components Over High
979 Mountain Asia, *Frontiers in Earth Science*, 7, 120, <https://doi.org/10.3389/feart.2019.00120>, 2019.

980